International Journal of Applied Earth Observations and Geoinformation 110 (2022) 102810

Contents lists available at ScienceDirect

International Journal of Applied Earth Observations and Geoinformation

journal homepage: www.elsevier.com/locate/jag

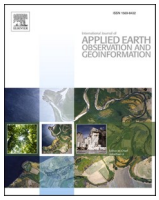

# Satellite product to map drought and extreme precipitation trend in Andalusia, Spain: A novel method to assess heritage landscapes at risk

M. Moreno [a,*], C. Bertolín [b], P. Ortiz [a], R. Ortiz [a]

[a] Department of Physical, Chemical and Natural Systems, Pablo de Olavide University, Carretera de Utrera Km 1, ES-41013 Seville, Spain
[b] Department of Mechanical and Industrial Engineering, Norwegian University of Science and Technology, Norway

ARTICLE INFO

*Keywords:*
Earth fortification
Mediterranean area
Remote sensing
Torrential rains
Drought
Risk
Geo big data

ABSTRACT

The objective of this work is to develop a methodology for the identification of extreme rain and drought events that have occurred in the last 30 years using products derived from satellite images.

Proposed methodology uses statistical reducers such as percentile, drought indexes, and map algebra at a geo big data scale. The daily precipitation data from the *Precipitation Estimation from Remotely Sensed Information Using Artificial Neural Networks-Climate Data Record* and *Climate Hazards Group InfraRed Precipitation with Station Data* were validated by comparison with ground station data. Extreme event maps were obtained from the use of high percentiles. Drought maps were obtained from the standardized precipitation index using low percentiles.

The data were migrated to a geographic information system that allows interrelation with other geographic data. Its application to the study of the fortifications preserved in Andalusia classified all structures according to the level of exposure to these dangers and identified two areas of precipitation with different characteristics according to the influence of existing teleconnection patterns.

Applied to the study of heritage landscapes, this methodological model minimizes the uncertainty associated with the use of satellite precipitation products, facilitates the planning of preventive conservation activities, and the management of existing resources in occurrence of extreme events.

## 1. Introduction

In recent years, there has been a growing interest in the use of remote sensing in many different disciplines (Barmpoutis et al., 2020; Gao et al., 2020; Holloway and Mengersen, 2018; Weiss et al., 2020). This growth reflects the substantial changes that have occurred in the production and availability of satellite images, channels of information in open access, potential interested users, and broadening of analysis methodologies (Ghamisi et al., 2019). To date, thousands of satellites have been sent into space to gather accurate and relevant data useful for scientific research, weather predictions and climate and environment monitoring. Consequently, remote sensing generates terabytes of information daily that is sent from the satellites to ground data stations (Ma et al. 2015; Chuvieco & Emilio 2007; Toth & Jóźków 2016; Kumar & Mutanga 2018; Chuvieco 2016).This has modified the fundamentals of the space system and services associated with remote sensing and has led some authors to identify a paradigm shift and theorize about the opportunities offered by this changing situation (Denis and Pasco, 2015).

As a result, in recent years new analysis methods and software have emerged that allow working with large volumes of data (Mutanga and Kumar, 2019; Wang et al., 2016). Although desktop software does not allow working with complete satellite series, working in the cloud offers affordable services. The Google Earth Engine® (GEE) computing platform is an example of these emerging tool (Google Developers: Get Started with Earth Engine, 2022). The processing in the cloud using an Application Programming Interface (API) and a code editor based on JavaScrip and/or Python language makes it possible to massively analyze series of satellite images from a personal computer (Gorelick et al., 2017; Kumar and Mutanga, 2018; Mutanga and Kumar, 2019). GEE opens the possibility of jointly analyzing the satellite images available since 1980, working with historical series and analyzing global environmental phenomena, changes, and trends (Ma et al., 2015; Mutanga and Kumar, 2019; Wang et al., 2016).

In the management of cultural heritage, this new way of detecting, analyzing, and therefore, understanding the space (globally) offers both new challenges and available resources for the management of cultural heritage landscapes (Cuca and Hadjimitsis, 2019). Cultural landscapes are the result of natural and anthropic modifications of territory and have ecological, environmental, and social significance (Rossler, 2006)

* Corresponding author.
*E-mail address:* mmorfal@upo.es (M. Moreno).

https://doi.org/10.1016/j.jag.2022.102810
Received 17 December 2021; Received in revised form 16 April 2022; Accepted 2 May 2022
Available online 11 May 2022

**Nomenclature**

*Acronyms*

| | |
|---|---|
| AEMET | State Meteorological Agency of Spain |
| CDF | cumulative density function |
| CHIRPS | Climate Hazards Group InfraRed Precipitation with Station Data |
| CLC | Corine Land Cover |
| EATL | East Atlantic |
| GEE | Google Earth Engine |
| GIS | Geographic Information System |
| GLDAS | Global Land Data Assimilation System |
| GRACE | Gravity Recovery and Climate Experiment |
| GSMaP | Global Satellite Mapping of Precipitation |
| LIDAR | Light Detection and Ranging |
| MIRAS | Microwave Imaging Radiometer using Aperture Synthesis |
| MO | Mediterranean Oscillation |
| NAO | North Atlantic Oscillation |
| PERSIANN | Precipitation Estimation from Remotely Sensed Information Using Artificial Neural Networks-Climate Data Record |
| PR | precipitation radar |
| RP | reference period |
| SAR | synthetic aperture radar |
| SMOS | Soil Moisture and Ocean Salinity |
| SPI | Standardized precipitation index |
| TRMM | Tropical Rainfall Measuring Mission |
| UAV | unmanned aerial vehicle |
| WeMO | West Mediterranean Oscillation |
| WMO | World Meteorological Organization |
| WRUS | West Russia |

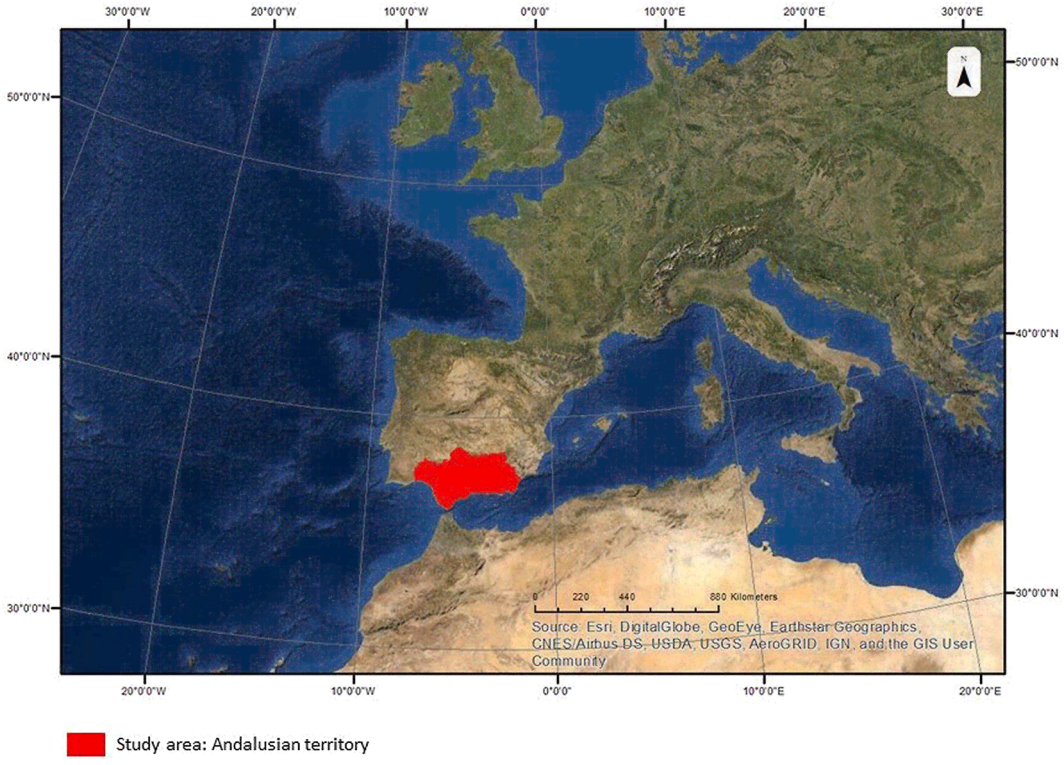


**Fig. 1.** Location of the Andalusia region, South of Spain. Base maps from EsriDigitalGlobe.

Cultural landscapes are not only resources that favor sustainable development of the populations that inhabit them, in addition they offer capability of mitigating and adapting to ongoing climate change (Bonazza et al., 2021; Cacciotti et al., 2021; Wilson, 2019). The recent growing interest in the protection of cultural landscapes has been accompanied by the development of international letters and recommendations that highlight the need to ensure long-term preservation through the development of monitoring management tools and strategies (Dastgerdi et al., 2019; Taylor et al., 2014; Council of Europe, 2009; UNESCO., 2020).

In this context, the remote sensing analysis technique hold great potential as it allows:

- recovering information over a long period of time (i.e., decades),
- monitoring at global/national/regional/local and district scales with very low economic cost,
- data collection without interfering with the terrain being investigated (i.e., non-destructive technique).

Despite these potentialities, the number of articles that use remote sensing as an analysis technique in the heritage field is limited. Existing studies have researched the prospecting of archaeological sites (Luo et al., 2019; Hadjimitsis et al., 2020), the analysis of risk in heritage structures (Abate & Lasaponara, 2019; Agapiou et al., 2020; Cuca, 2017), and the sustainable management of urban and non-urban landscapes (Agapiou et al., 2015; Hadjimitsis et al., 2013; Wellmann et al., 2020; Xiao et al., 2018). Although passive sensors and multispectral images are the most used tools, in the last 10 years, there has been a

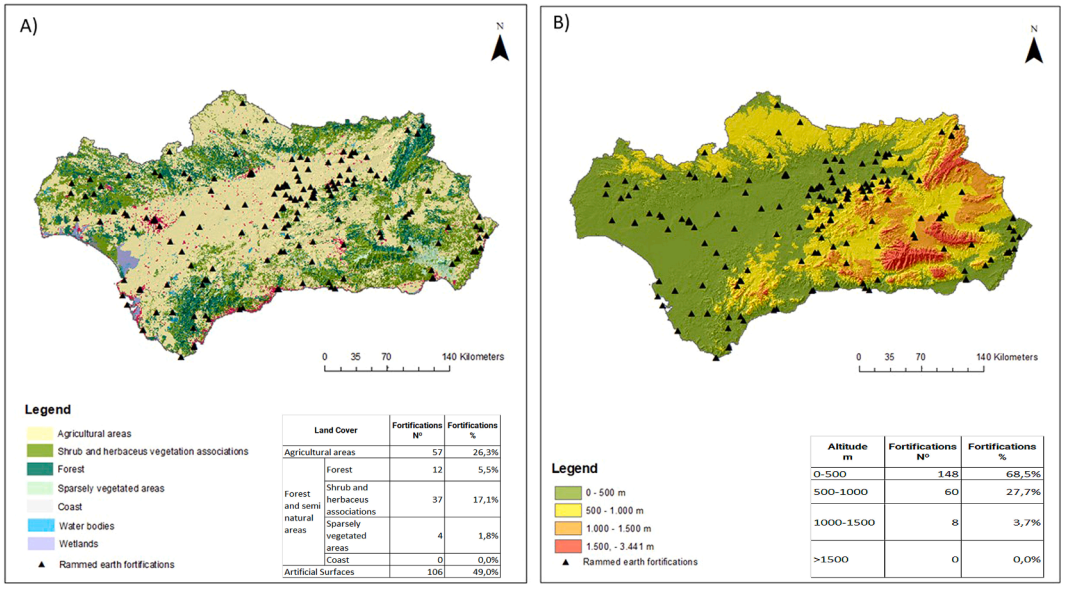


**Fig. 2.** A) Land cover map in Andalusia indicating the distribution of fortifications (black triangles). (Based on data from the Corine Land Cover). B) Altitude range for the Andalusia with the distribution of preserved fortifications (black triangles). (Based on data from the Shuttle Radar Topographic Mission: SRTM 30).

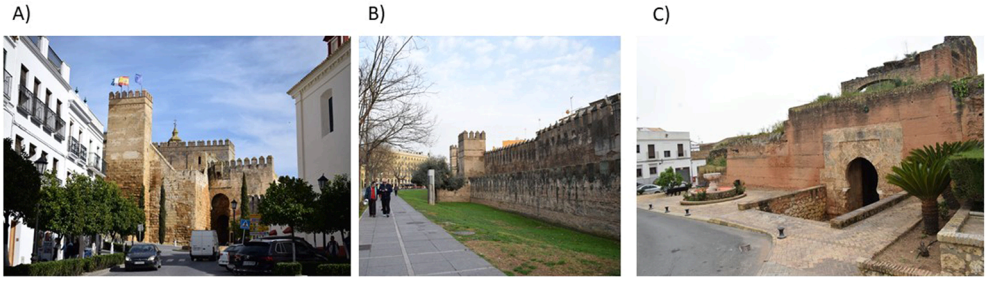


**Fig. 3.** Examples of medieval rammed earth fortification preserved in the Andalusian Region in Spain: A) Carmona, B) Sevilla C) Niebla., Image taken by Moreno M., 2021.

**Table 1**
Classified SPI values.

| SPI values | Cualitative scale |
|---|---|
| >2.00 | Extremely humid |
| 1.50 to 1.99 | Very humid |
| 1.00 to 1.49 | Moderately humid |
| –0.99 to 0.99 | Normally |
| –1.00 –1.49 | Moderately dry |
| –1.50 –1.99 | Very dry |
| < –2.00 | Extremely dry |

gradual increase in the use of high spatial resolution tools as Light Detection and Ranging (LIDAR), and radar satellites (synthetic aperture radar: SAR). These tools are used in combination with other geo-informatics techniques, such as Geographic Information System (GIS), laser scanning, and unmanned aerial vehicle (UAV) (Ambrosia et al., 2019; Luo et al., 2019; Themistocleous, 2020).

Analyzing the methodological approach used to process data in past cultural heritage studies it reveals that most authors worked with a limited number of satellite images by downloading and processing raw data. This means that the use of satellite images on a big data scale, despite being widespread in other fields, is scarce in cultural heritage. Pioneering works using this type of methodology were those by Agapiou, Levin and Elfadaly (Agapiou and Lysandrou, 2021; Elfadaly et al., 2022; Levin et al., 2019), although most published articles only explained the possibilities that this novel method could offer in the future in risk management (Agapiou, 2017; Wang & Luo, 2020) and in environmental and climatic control of heritage landscapes (Lasaponara & Masini 2020).

Despite the availability of data, knowledge, and resources, this methodological gap has delayed and hindered the development of studies to analyze global phenomena in cultural landscapes using historical satellite data. This situation is specially worrying in the case of the development of studies that analyze the environmental risks that may impact cultural landscapes in the context of climate change.

Changes in temperature, precipitation patterns, droughts, and heavy rain events are expected to pose a major risk for the conservation of heritage assets (Aktas 2021; Brimblecombe, Grossi, & Harris 2011; Carroll & Aarrevaara 2018; Fatorić & Seekamp 2017; Gandini, et al. 2017; Orr et al. 2021; Sesana et al. 2021). Most of these studies discussed the necessity of obtaining reliable climatic data that interrelate with vulnerability data (Phillips 2015) without explaining in detail where to obtain these climatic data or how to use them to retrieve information regarding the vulnerability over a specific territory (Gandini et al. 2017). The few published climate forecasts and re-analyses have low spatial resolution and did not have access to raw data (Cagigas et al. 2020; Sabbioni et al. 2010). Although they are useful for understanding the possible effects associated with climatic change, they are too general and further studies should be completed to develop tools for the collection of climate and hazard data. Therefore, indices or thresholds obtained from satellite product analysis, that offer a practical solution to collect meteorological data over specific heritage landscapes, should be

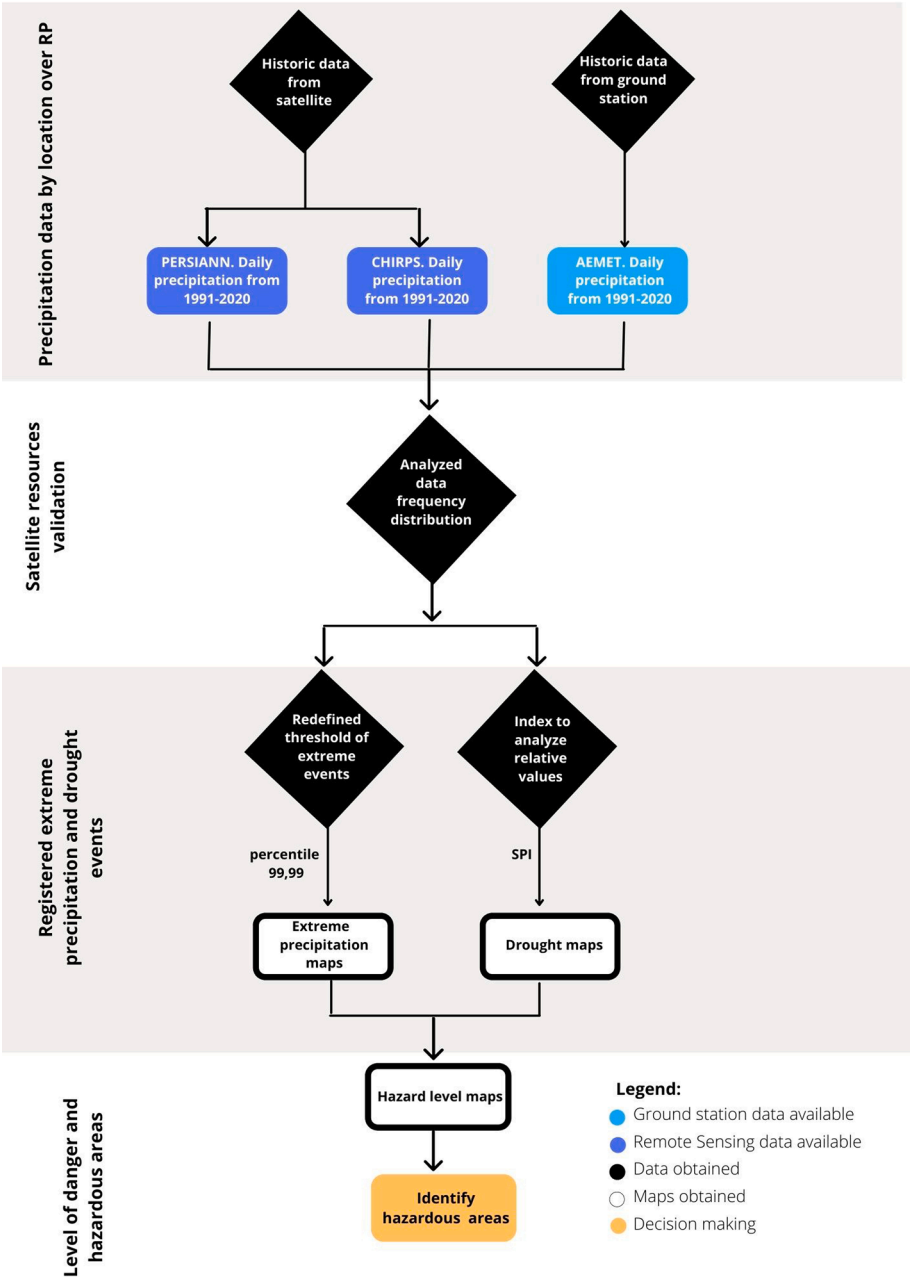


**Fig. 4.** Methodological process.

correlated with vulnerability indices with the help of heritage management specialists, restorers, and architects.

In this context, the novelty of this study is the use of statistical analysis methodologies on satellite images to assess climatic hazards in specific heritage sites. The study objects analyzed are drought and extreme precipitation.

Drought is a natural phenomenon caused by decreases in precipitation that induce a hydrological, meteorological, and socioeconomic imbalance (Peña et al., 2016). Droughts have complex environmental impacts that can affect numerous ecosystem components. Since the mid-20th century, studies have reported the use of drought indices based on the analysis of precipitation, temperature, soil moisture, and health of vegetation (Heim 2002; Zargar et al. 2011). Since the availability of satellite images (i.e., beginning of the 21st century) (Jiao et al. 2021; Liu et al. 2020; West et al. 2019) droughts have been studied using the satellite products:

- precipitation by Global Satellite Mapping of Precipitation (GsMaP) or Tropical Rainfall Measuring Mission (TRMM).
- temperature as by Moderate Resolution Imaging Spectroradiometer (MODIS) and Advanced Spaceborne Thermal Emission and Reflection Radiometer (ASTER).
- soil moisture by Soil Moisture Active Passive (SMAP) or by Soil Moisture and Ocean Salinity (SMOS).
- groundwater by Gravity Recovery and Climate Experiment (GRACE).
- evapotranspiration by MODIS and Global Land Data Assimilation System (GLDAS).
- vegetative vigor by MODIS and Landsat.

More recently, new instruments onboard satellites, such as Synthetic Aperture Radar (onboard the Sentinel 1), Microwave Imaging Radiometer using Aperture Synthesis (MIRAS onboard the SMOS), radar altimeter (onboard the JASON-3), or the many tools constituting the gravimetric satellite GRACE have been implemented (Lopez et al. 2020;

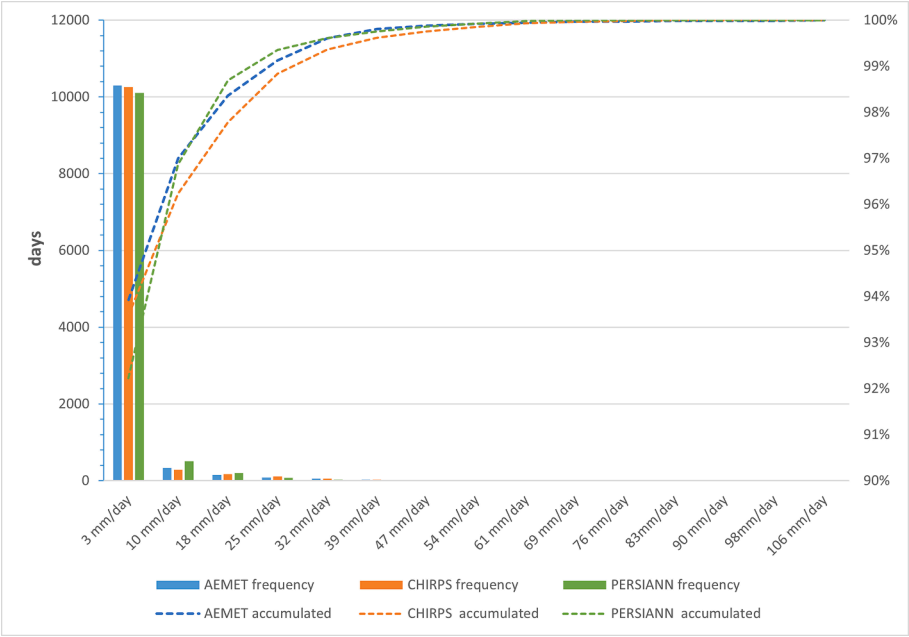


**Fig. 5.** Cumulative distribution function of daily precipitation data (right y-axis) averaged over the 1991–2020 period as collected by AEMET, CHIRPS, and PERSIANN. Frequency of daily precipitation thresholds (histograms on the left y-axis) as calculated for AEMET (blue), CHIRPS (orange), and PERSIANN (green). (For interpretation of the references to color in this figure legend, the reader is referred to the web version of this article.)

**Table 2**
Percentiles, precipitation threshold, occurrence and return period at the Seville Airport location as obtained by CHIRPS.

| Precipitation registers in Seville airport (CHIRPS; 1991–2020) | | | | |
|---|---|---|---|---|
| **Percentiles** | **Precipitation amount (mm/day)** | **Accumulated Events (rain days)** | **Cumulative Probability** | **Return Period (day)** |
| 92.22 | 0 | 10,958 | 100% | 1 |
| 95.71 | 7 | 852 | 7.775% | 13 |
| 98.68 | 16 | 263 | 2.400% | 42 |
| 99.44 | 26 | 88 | 0.803% | 125 |
| 99.70 | 35 | 47 | 0.428% | 233 |
| 99.90 | 49 | 16 | 0.146% | 685 |
| 99.95 | 54 | 10 | 0.091% | 1096 |
| 99.97 | 59 | 6 | 0.054% | 1826 |
| 99.98 | 64 | 3 | 0.027% | 3653 |
| 99.99 | 68 | 2 | 0.018% | 5479 |
| 100.00 | 72 | 1 | 0.009% | 10,958 |

Vishwakarma 2020). Additionally, there is also a great interest in the massive recovery and analysis of historical satellite series using machine learning, big data, algorithms, and scripts (AghaKouchak et al. 2015; Balti et al. 2020; Jiao et al. 2021; Sahoo et al. 2015; Xu et al. 2016).

Extreme precipitation events are characterized by rainfall exceeding a specific threshold, commonly expressed in percentiles, to make them exceptional events (Camuffo et al.2020; Schär et al. 2016; World Meteorological Organization 2016). In heritage landscapes, extreme precipitation events can generate floods and are one of the main causes of degradation (Figueiredo et al.2020; Maierhofer et al. 2008). Extreme precipitation studies in the literature are based on data collected both from ground meteorological stations and satellite resources. The most widely used resources are TRMM, GsMaP, Climate Hazards Group InfraRed Precipitation with Station data (CHIRPS), and climate reanalysis datasets like ERA-5 or Precipitation Estimation from Remotely Sensed Information Using Artificial Neural Networks-Climate Data Record (PERSIANN) (Michaelides et al. 2009; Sun et al. 2018).

Within this framework, this study proposes the use of satellite resources to map the drought and extreme precipitation trends in Andalusia, Spain (Mediterranean area) over the last 30 years and it evaluates how these factors condition the conservation of the rammed-earth fortifications preserved there.

## 2. Earth fortifications in the Andalusian territory, Spain

Located within the Mediterranean area, the Andalusian territory is in the south of the Iberian Peninsula, bounded by the Atlantic Ocean to the west, and the Mediterranean Sea to the east (Fig. 1). With a location at latitude 37° 00′ N and longitude 3° 50′ W, its climate is strongly influenced by subtropical anticyclones and shows marked differences during mild-humid winters and very dry summers (Fernanda & López 2003; Gómez-Zotano et al. 2015). According to the Köppen climate classification, Western Andalusia has a temperate climate with a markedly dry and hot summer while Eastern Andalusia has a dry cold steppe climate with small areas of warm deserts located in Almería (Ministerio de Medio Ambiente, 2011). The altimetric differences and the effects of the two different water masses present during the seasons give rise to different climatic sub-regions. Based on these aspects, Gomez-Zotano et al. (2015) proposed a division of Andalusia into five climatic sub-regions: coastal, interior, mid-mountain, high mountain, and south-eastern climates. Coastal climates are influenced to a greater degree by ocean influence than inland climates, while medium and high mountain zones have lower temperatures. Unlike temperature, the precipitation values show strong oscillations within the same region.

Fig. 2 shows the land cover types in Andalusia. Agricultural areas (light yellow in Fig. 2a), located in the valley of the Guadalquivir River (less than500 m a.m.s.l.) are the predominant type of coverage. Forests and semi-natural environments at higher altitudes (>500 m.a.m.s.l.) are largely located in the mid-mountains (green color in Fig. 2a). Within this group, scrub areas are the most frequent and include a great variety of ecosystems, such as steppes, plains, and scrublands. While artificial surfaces (i.e., cities and towns) are located mainly in the provincial capitals and coastal areas.

Medieval rammed-earth fortifications are an essential characteristic of the historical landscape within Andalusia (Fig. 3). According to the digital guide of the Cultural Heritage of Andalusia (https://guiadigital.iaph.es), the remains of 216 medieval walls or fortresses are preserved

| Precipitation distribution in Seville airport (CHIRPS, 1991-2020) | | | | | | | | | | | | | |
|---|---|---|---|---|---|---|---|---|---|---|---|---|---|
| Year/Month | January (mm) | February (mm) | March (mm) | April (mm) | May (mm) | June (mm) | July (mm) | August (mm) | September (mm) | October (mm) | November (mm) | December (mm) | Year/Accumulated mm |
| 1991 | 20.42 | 106.63 | 96.92 | 34.01 | 15.98 | 9.77 | 0.00 | 0.00 | 52.57 | 116.55 | 54.23 | 61.22 | 568.30 |
| 1992 | 25.33 | 40.91 | 28.41 | 56.92 | 20.16 | 18.27 | 0.00 | 0.00 | 29.82 | 94.50 | 20.95 | 17.21 | 352.47 |
| 1993 | 45.66 | 29.59 | 43.38 | 63.92 | 56.42 | 11.63 | 0.00 | 5.03 | 19.72 | 147.93 | 92.05 | 13.43 | 528.76 |
| 1994 | 40.19 | 48.48 | 11.65 | 40.83 | 56.76 | 9.81 | 0.00 | 0.00 | 11.37 | 41.55 | 89.56 | 11.41 | 361.62 |
| 1995 | 19.59 | 49.25 | 25.39 | 34.08 | 11.93 | 7.51 | 2.81 | 4.37 | 8.61 | 14.26 | 97.78 | 222.46 | 498.05 |
| 1996 | 298.43 | 69.60 | 34.18 | 46.38 | 61.20 | 8.88 | 0.00 | 0.00 | 31.38 | 30.16 | 49.84 | 337.73 | 967.77 |
| 1997 | 202.19 | 0.00 | 6.28 | 38.24 | 48.14 | 14.04 | 0.00 | 7.31 | 49.82 | 39.47 | 182.80 | 160.92 | 749.21 |
| 1998 | 77.35 | 38.59 | 34.05 | 43.35 | 53.90 | 6.56 | 0.00 | 0.00 | 38.31 | 10.56 | 36.46 | 43.70 | 382.83 |
| 1999 | 56.74 | 11.58 | 49.62 | 28.69 | 20.16 | 9.71 | 0.00 | 0.00 | 36.96 | 178.16 | 33.24 | 61.22 | 486.07 |
| 2000 | 52.37 | 0.00 | 20.32 | 143.77 | 92.72 | 5.61 | 0.00 | 0.00 | 21.21 | 41.00 | 85.90 | 61.22 | 524.12 |
| 2001 | 132.08 | 25.54 | 94.80 | 12.02 | 32.95 | 4.54 | 3.01 | 4.26 | 50.01 | 64.48 | 102.51 | 58.47 | 584.66 |
| 2002 | 35.41 | 11.69 | 84.74 | 67.35 | 18.78 | 9.87 | 0.00 | 0.00 | 78.45 | 25.16 | 136.51 | 59.75 | 527.70 |
| 2003 | 51.37 | 59.27 | 44.70 | 129.64 | 13.19 | 5.78 | 0.00 | 0.00 | 32.57 | 186.65 | 105.45 | 125.96 | 754.59 |
| 2004 | 19.87 | 83.95 | 46.49 | 49.48 | 76.40 | 5.27 | 0.00 | 0.00 | 6.66 | 85.52 | 23.68 | 42.06 | 439.35 |
| 2005 | 4.73 | 38.32 | 35.00 | 21.98 | 27.05 | 0.00 | 0.00 | 0.00 | 7.13 | 97.85 | 53.28 | 23.83 | 309.17 |
| 2006 | 103.61 | 48.95 | 62.74 | 48.91 | 22.67 | 18.25 | 2.83 | 5.01 | 33.46 | 135.21 | 129.18 | 35.95 | 646.78 |
| 2007 | 38.99 | 57.59 | 26.49 | 57.99 | 60.02 | 8.76 | 0.00 | 7.49 | 59.51 | 40.74 | 102.46 | 36.70 | 496.72 |
| 2008 | 53.85 | 65.19 | 20.41 | 131.02 | 33.58 | 0.00 | 2.42 | 0.00 | 46.41 | 93.38 | 47.35 | 52.50 | 546.09 |
| 2009 | 65.12 | 94.06 | 48.87 | 41.14 | 13.23 | 7.81 | 0.00 | 0.00 | 36.15 | 27.97 | 36.82 | 220.59 | 591.75 |
| 2010 | 153.80 | 239.50 | 91.15 | 64.83 | 17.01 | 20.35 | 0.00 | 0.00 | 18.37 | 59.20 | 104.60 | 197.23 | 966.02 |
| 2011 | 52.85 | 58.06 | 57.09 | 102.74 | 20.72 | 6.26 | 0.00 | 27.66 | 2.01 | 69.46 | 76.09 | 9.35 | 482.30 |
| 2012 | 27.36 | 0.00 | 17.62 | 50.70 | 26.51 | 7.24 | 0.00 | 0.00 | 55.45 | 92.83 | 111.00 | 37.26 | 425.97 |
| 2013 | 50.50 | 46.75 | 120.98 | 45.58 | 11.79 | 8.22 | 0.00 | 0.00 | 29.29 | 78.38 | 14.09 | 53.06 | 458.63 |
| 2014 | 69.05 | 72.56 | 55.04 | 34.84 | 15.37 | 9.72 | 1.36 | 0.00 | 36.08 | 80.37 | 166.14 | 47.92 | 588.44 |
| 2015 | 63.65 | 6.64 | 24.61 | 52.23 | 9.75 | 6.35 | 0.00 | 0.00 | 18.12 | 117.73 | 0.00 | 25.08 | 324.15 |
| 2016 | 55.10 | 38.01 | 22.74 | 70.38 | 102.73 | 0.00 | 0.00 | 0.00 | 12.16 | 107.23 | 119.94 | 65.33 | 593.62 |
| 2017 | 22.52 | 75.53 | 37.89 | 38.61 | 30.32 | 5.06 | 1.48 | 7.00 | 10.53 | 11.29 | 57.84 | 40.17 | 338.24 |
| 2018 | 81.33 | 44.07 | 77.91 | 91.58 | 23.74 | 6.18 | 0.00 | 3.66 | 22.79 | 83.45 | 74.24 | 18.41 | 527.37 |
| 2019 | 37.34 | 13.30 | 9.93 | 114.45 | 7.34 | 2.68 | 0.00 | 0.00 | 14.98 | 21.17 | 83.61 | 84.86 | 389.65 |
| 2020 | 58.43 | 7.07 | 34.58 | 55.85 | 40.64 | 4.69 | 0.84 | 0.00 | 28.30 | 26.02 | 99.93 | 36.28 | 392.63 |
| Month average | 67.17 | 49.36 | 45.47 | 60.38 | 34.70 | 7.96 | 0.49 | 2.39 | 29.94 | 73.94 | 79.58 | 75.38 | 526.77 |

**Fig. 6.** Precipitation occurrence over the 1991–2020 period for the Seville Airport location. Data obtained by CHIRPS. In red months and years with higher precipitation, in orange with medium range precipitation, and in green with lowest precipitation. (For interpretation of the references to color in this figure legend, the reader is referred to the web version of this article.)

(black triangles in Fig. 2). To understand their current role within the region and in several urban contexts, their significance in terms of historic, cultural, social, and identity value must be considered in addition to their potential in attracting tourism and employment. Castles, ramparts, and towers made of rammed earth are exposed to the elements, and the changing climatic conditions affect their long-term conservation (Beckett et al. 2020; Avram et al, 2001.).

## 3. Resource data and methods

To analyze the precipitation patterns of Andalusia, a very recent reference period (RP) of 30 years was selected (1991–2020).

Precipitation data were obtained from two different satellite resources: PERSIANN and CHIRPS. Although there are other satellite resources to evaluate rainfall, such as GPM and GSMaP they only have data since 2000, which makes it impossible to use them to analyse climatic normal period based on 30-years data. Other resources like Terra Climate offer only one image per month, which makes it impossible to use them to analyze extreme events that happens to daily temporal scale.

PERSIANN is a daily quasi-global precipitation product from 1983 to present with a spatial resolution of 0.25° (approximately 27 × 27 km). From infrared satellite images, the PERSIANN algorithm can calculate the intensity of rain on the Earth's surface (Hsu et al., 2021).

CHIRPS is obtained from TRMM constellation satellites and historical ground stations. It offers a daily product, from 1981 to the present, with a spatial resolution of 0.05° (approximately 5 × 5 km) (Funk et al., 2015).

The historical series of both satellite resources were analyzed on a big data scale using GEE. The developed scripts made it possible to jointly analyze 10,000 satellite images and obtain daily precipitation data for the entire Andalusian region over the RP (30 years).

Because the estimation of rainfall by satellite is subject to errors due to the non-direct relationship between the observed and calculated variables, it is necessary to validate the models before use. To validate the reliability of the satellite data analyzed, they were compared with data collected by a reference ground station. The ground station used is located at Seville Airport (Lat. 37° 25′ 0″ N - Long. 5° 52′ 45″ W, and altitude 34 m. a.m.s.l.). It is a complete ground weather station owned by the State Meteorological Agency of Spain (AEMET) in accordance with the provisions of the World Meteorological Organization (WMO). The data collected by CHIRPS and PERSIANN for the same coordinates were downloaded using scripts from the GEE. The frequency distributions of these three different meteorological resources were then compared.

The cumulative density function (CDF) of the daily precipitation values over the RP were calculated from the ground weather station and two satellite resources. Then CDF was compared with the ground weather station to evaluate the precision and accuracy of the satellite resources analyzed.

A percentile is the data relating to the $n^{th}$ value obtained by dividing an assigned set of n linearly ordered data, so that the number of values less than h constitutes a given percentage of n. Using percentiles as statistical reducers, maps of extreme rainfall events were obtained from the analysis of the CHIRPS and PERSIANN satellite images in GEE. This analysis was carried out on the 10,958 satellite images available from 1991 to 2020.The 99.9th and 99th percentile maps were used to identify the areas where the strongest precipitation events have accumulated over the RP. Based on the highest percentile maps, a daily rainfall amount threshold in millimeters was determined to define extreme precipitation events.

The results obtained for each pixel of the Andalusia territory were further classified into five ranges according to the $mm/m^3$ fallen on the rainiest days. The pixel values over the 290 locations where fortifications were located were extracted. This allowed classifying the fortifications' site according to the heavy rain hazard (very low, low, acceptable, high, and very high danger).

Then, the Standardized Precipitation Index (SPI) was calculated over the RP annually. SPI represents the number of standard deviations by which the observed variable deviates from the long-term mean for a normally distributed random variable (Guttman 1999; McKee et al. 1993).

$$SPI(j) = (\Sigma xj - \overline{X}\, j(z))\ \sigma xj(z).$$

Σxj: sum of daily precipitation over the jth time step (j equals to 12 months).

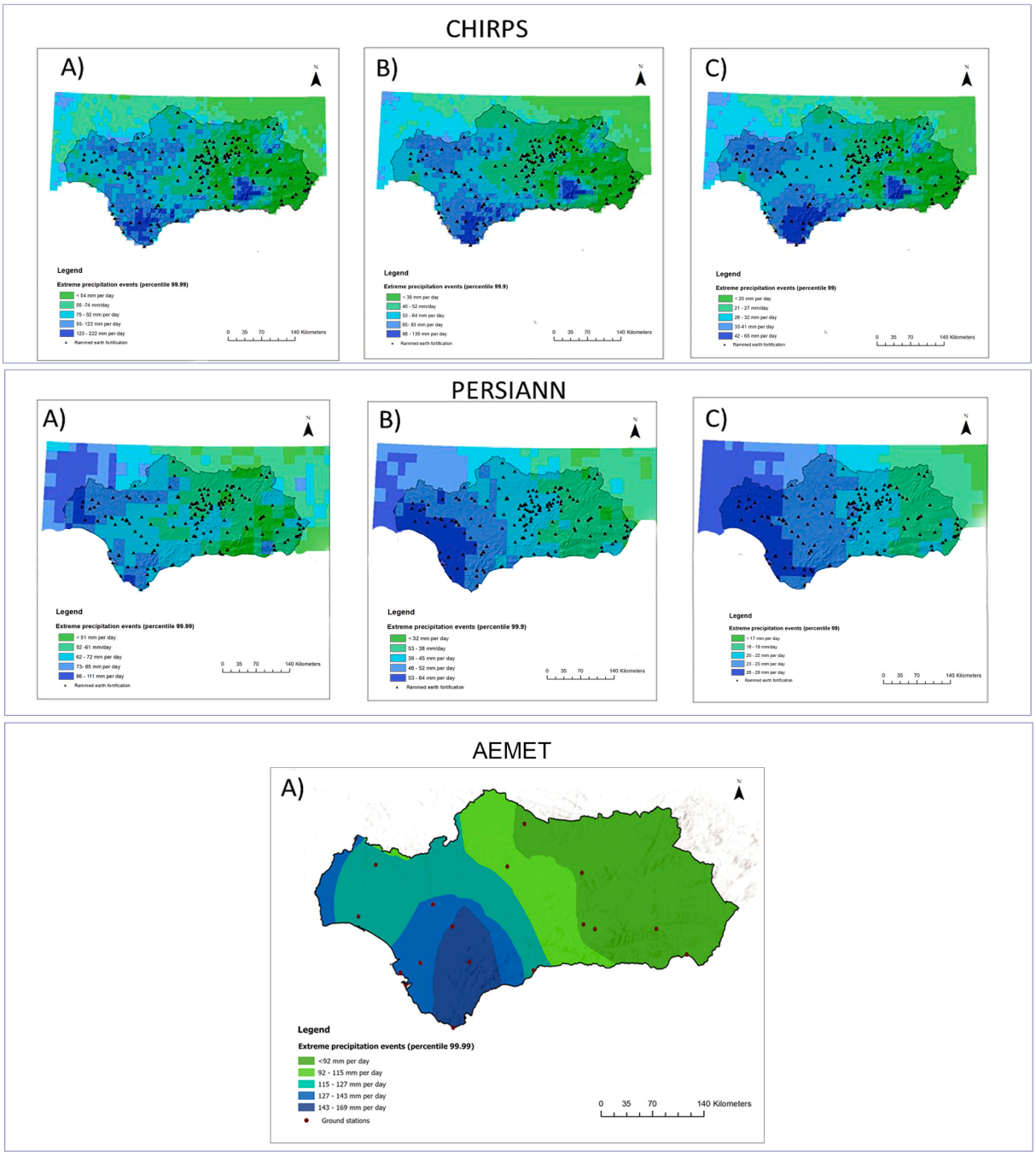


**Fig. 7.** Classification of Andalusian territory according to the threshold of extreme precipitation events. A) 99.99th threshold percentile; B) 99.90th percentile; C) 99.00th percentile. Data obtained from the CHIRPS (above) PERSIANN (in the middle) y AEMET (bellow).

$\overline{X}$ j: average daily precipitation over the jth time step (j = 12 months).
σxj: standard deviation of daily precipitation over the jth time step in a reference period.
z: reference period (30 years).

Because of its simplicity, this index is recommended for drought monitoring by the WMO (Organización Meteorológica Mundial, 2012). By using SPI, the historical precipitation distribution for the annual time steps were compared with the total precipitation for the RP. As a result, 30 annual SPI maps were obtained for the last 30 years. The SPI maps included in this study were calculated from the analysis of CHIRPS satellite images. The obtained SPI values were classified according to the Table 1 scale (Organizacion Meteorológica Mundial, 2012).

All the achieved and elaborated information was then migrated to a geographic information system. The fortifications were georeferenced using the digital guide of the cultural heritage of Andalusia (https://guiadigital.iaph.es). In total, the analyzed and elaborated data allowed the reconstruction of maps on extreme precipitation thresholds and periods of droughts for all the groups of 216 fortifications over the RP. Finally, these maps were classified according to a hazard scale from 1 to 5 to easily identify the most endangered areas that need disaster risk reduction prioritization actions. Fig. 4 shows a scheme of the methodological process described in this section.

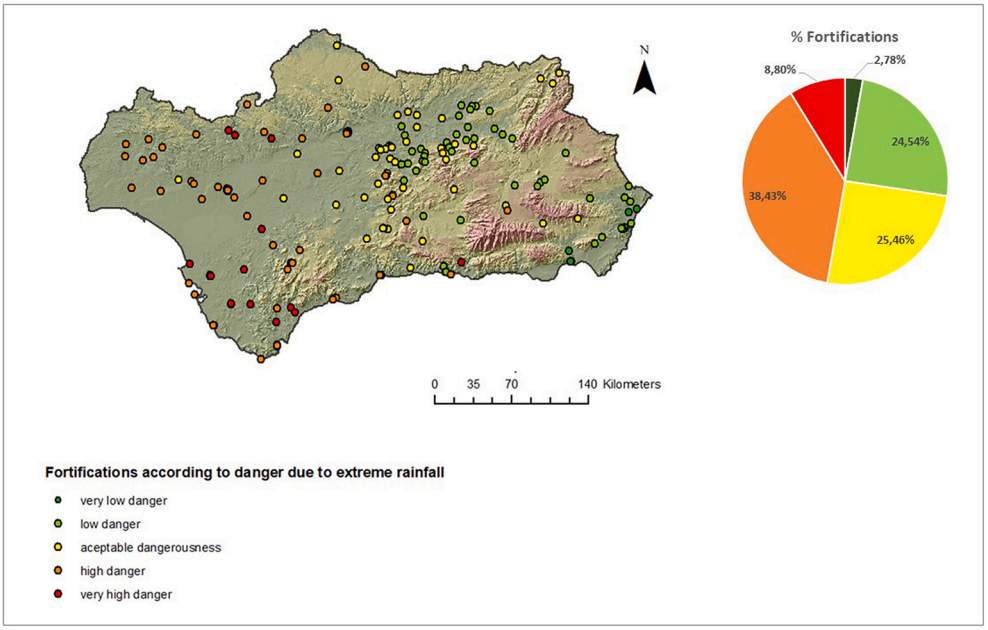


**Fig. 8.** Fortifications classified according to danger of extreme rainfall with a color code reported in the legend. The percentage of fortification at different danger level is also reported as pie chart on the top right.

## 4. Results and discussion

### 4.1. Validation

The data validation process was accomplished by comparing the CHIRPS and PERSIANN satellite resources with the data collected by the AEMET Seville Airport ground station over the RP.

Fig. 5 report the total data sample size (n = 10958), the absolute and cumulative distribution (i.e., %), the mark or threshold of the daily precipitation value per each reported percentile, and the further subdivision in intervals or range adopted for the extreme event classification. The three resources analyzed show a distribution strongly skewed to the right with similar peaks (i.e., >95% of the daily precipitation values are lower than 15 mm/day). These peaks indicate a high frequency of days without rain and, in the case of precipitation, the development of rainfall of weak or moderate intensity. In turn, in the three analyzed resources, less than 1% of the recorded data corresponded to precipitation values above 50 mm/day (i.e., heavy rainfall events).

Looking at the dispersion of the data, the precipitation threshold corresponding to a selected percentile changes according to the resource used (Fig. 5). The maximum value (i.e., 100th percentile) collected in the AEMET was 106.40 mm/day, in CHIRPS it ranged between 80.00 and 87.00 mm/day, while in PERSIANN between 65.00 and 73.00 mm/day. These data reflect a tendency in satellite resources to underestimate precipitation values in the case of torrential rain occurrences. Of the two satellites analyzed, PERSIANN showed the least dispersion and thus, a greater tendency to underestimate the data collected during heavy rainfall events.

In general, the analysis showed that the precision of the collected data was acceptable, with a discrepancy in accuracy by up to 31 mm/day. Therefore, although satellite resources provide data regarding the distribution of rainfall with continuous spatial and temporal coverage, however it is necessary to redefine their thresholds based on reliable calibrations from the ground stations.

In addition to the rainfall threshold at high percentiles (>99th percentile), the return period of such extreme occurrences was assessed at specific geographical points. The return period is one of the most important hydrological variables in the analysis of extreme events. It is based on the statistical record of the past and allows the prediction and determination of the probability of risk (i.e., frequency of occurrences). The longer the return period, the lower is the probability of an event occurring.

Table 2 shows the cumulative probability and return period for the highest percentiles obtained by elaborating the data collected by the CHIRPS satellite. The 99th percentile represents the top 1% heaviest precipitation events identified with a threshold of rainfall higher than 21.00 mm/day. Over the analyzed RP, 145 events with these characteristics were registered, giving a return period of 76 days. The 99.90th percentile records precipitation events above a threshold of 49.00 mm/day. Over the RP, 16 events were registered, giving a return period of one event every 2 years. Finally, the 99.99th percentile registers events above 68.00 mm/day. Over the 1991–2020 period, only two events with these characteristics were registered, giving a return period of 15 years. Because an extreme event corresponds to extraordinary events, the 99.90th and 99.00th percentiles were used to prepare maps of the heaviest rainfall events in Andalusia.

Fig. 6 shows the monthly distribution of precipitation events at Seville Airport over the RP. The data used were obtained from CHIRPS. The annual average rainfall was 526.77 mm. The rainiest months were the winter months (October, November, and December), presenting an average that oscillates between 73.94 and 75.38 mm/month. July and August were the driest months, with an average of less than 3.00 mm/month. In turn, the years with more annual accumulated precipitation were 1996 and 2010. As Fig. 6 shows, the results obtained from the analysis of the data collected by CHIRPS are very similar to the normal climatic values offered by the AEMET based on the data collected by the ground station (https://www.aemet.es/es/serviciosclimaticos/datosclimatologicos).

### 4.2. Data analysis

#### 4.2.1. Extreme precipitation events and their occurrences

The precipitation regime of Andalusia is generally moderate, with high interannual variability and heavy rainfall concentrated over few days alternated with long periods of no rain (Martinez-Artigas et al., 2021; Torelló-Sentelles and Franzke, 2021; Peña et al., 2016).

Percentile maps allow for better localization of heavy rainfall events

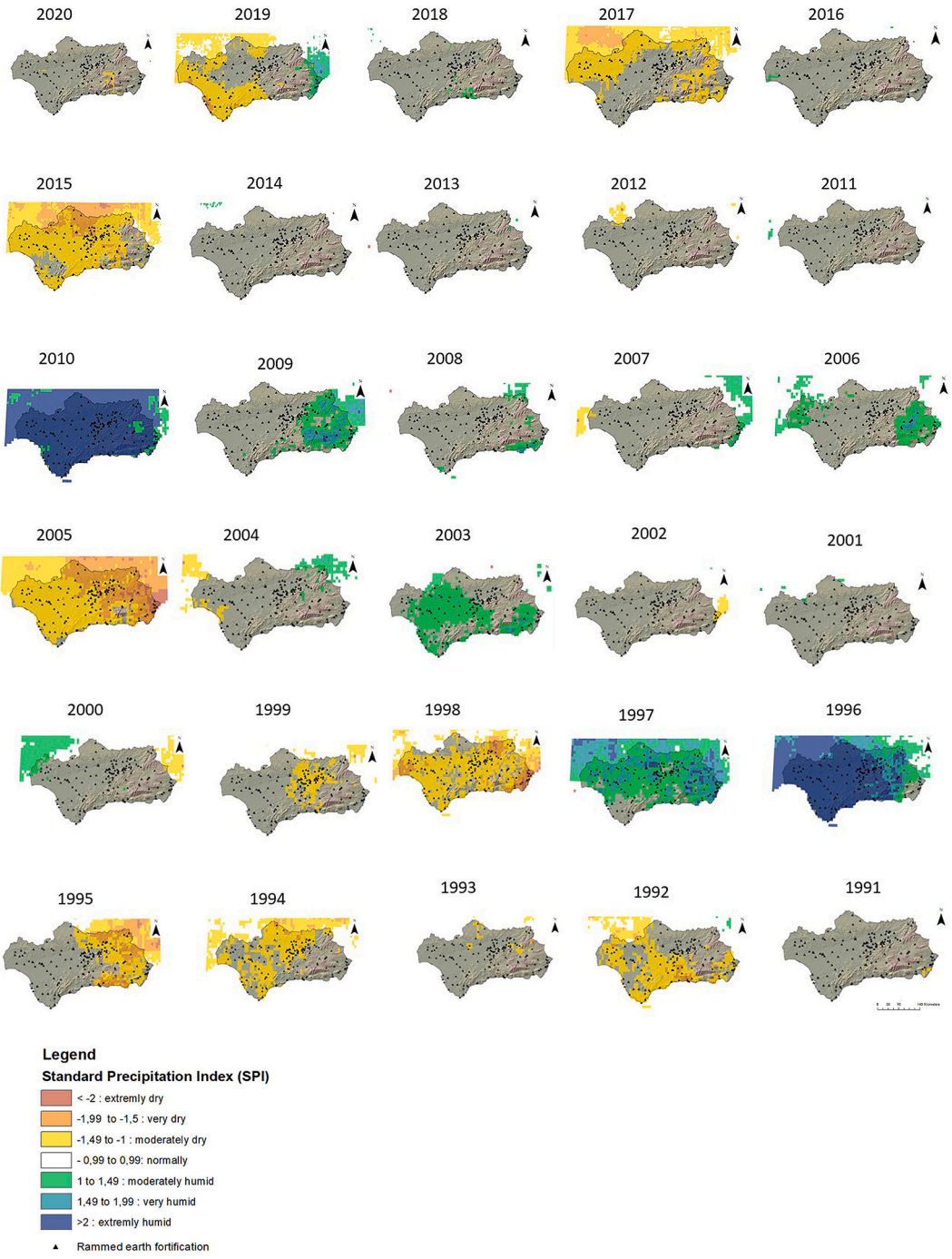


**Fig. 9.** Annual SPI reconstructed for each year over the reference period 1991–2020. Data obtained from CHIRPS. The SPI scale used to highlight risk is reported in the legend.

over the territory. Fig. 7 shows the risk maps obtained by the analysis of the 99.00th (Fig. 7a), 99.90th (Fig. 7b), and 99.99th (Fig. 7c) percentiles from the images available in CHIRPS and PERSIANN and the 99.99 th from the data available in AEMET. Although the thresholds vary considerably depending on the selected percentile at ground (99.00th percentile = 21.00 mm/day; 99.99th percentile = 68.00 mm/day) and with the selected satellite resource (PERSIAN 99.99th percentile = 85.00–111.00 mm/day; CHIRPS 99.99th percentile = 123.00–222.00 mm/day), the separation between areas with heavier extreme precipitations and those with weaker extreme events is equally detected over all the obtained percentiles maps. This clarifies the identification of the most endangered areas.

The maps over Andalusia can be split into two distinct zones depending on the strength of extreme rain events: the western side constitutes the zones of stronger extreme rain events over the RP, while the eastern side constitutes the zones of weaker extreme events. The highest mountains of the Sierra Nevada do not follow this trend; they are in the eastern zone but have heavy extremes. The spatial resolution of CHIRPS (5x5km) and Persiann (27x27 km) conditions the capability to identify differences between local factor and precipitation. According to the WMO (Organización Meteorológica Mundial, 2020), estimating meteorological variables at the local level requires a maximum separation between ground stations of 100 km. Thus, the spatial resolution of both satellite resources work within the admissible ranges. Despite this,

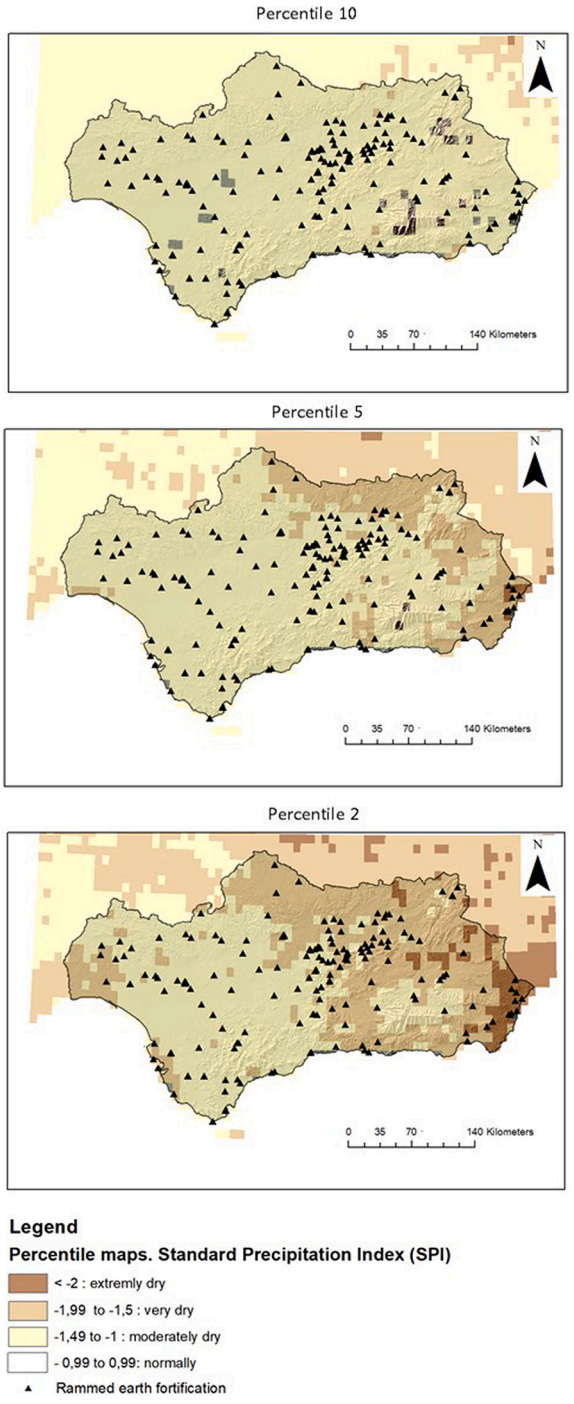


**Fig. 10.** Classification of Andalusia according to meteorological drought. A) 10th percentile of annual SPI; B) 5th percentile of annual SPI; C) 2nd percentile of annual SPI. The SPI scale used to highlight risk is reported in the legend.

to identify differences between the precipitation values on the coast, the valleys and the mountains it is recommended a maximum separation of 10 km between ground stations. In such a case, only CHIRPS works within the suggested ranges. Fig. 7 shows how in CHIRPS the altitude influences the occurrence of extreme precipitation but in PERSIANN not. The main reason is the scale threshold, that modify the observed geographic phenomena and the accuracy of the results (Quattrochi et al., 2017; Wu and Li, 2009).

Despite this, the magnitude of extreme rain events does not show a direct relationship with altitude in this study area..The identified western and eastern zones are subjected to the influence of teleconnection patterns. In the literature, several climatic indices have been used to detect the correlation between distant climatic events and evaluate how the natural variability of the climate influences local precipitation and temperature patterns. Numerous studies have related the effects of teleconnection patterns in the Iberian Peninsula with variability in rainfall (Casado et al. 2010; Criado-Aldeanueva & Soto-Navarro 2020; García-Barrón et al. 2018; Martin-Vide & Lopez-Bustins 2006; Martinez-Artigas et al. 2021).

Particularly interesting is the study carried out by Martinez-Artigas (2021), which analyzed the above correlations and obtained a regionalization that overlaps with the two zones differentiated in this study. In fact, in the western zone of Andalusia, the Atlantic flows penetrate without encountering obstacles until arriving at the Betic system. This western zone shows a good correlation with the North Atlantic Oscillation (NAO) and the Mediterranean Oscillation (MO) (Criado-Aldeanueva & Soto-Navarro 2020; Martinez-Artigas et al. 2021). The NAO is a North-South anomaly dipole with a north dipole centered in Greenland and south dipole centered in the Atlantic Ocean between 35 and 40° N, capable of detecting the strength and direction of western winds. It measures the difference in pressure at sea level that occurs between Iceland and the Azores. This index explains the trend of wind flow in North Atlantic. NAO (positive and negative) anomalies influence the temperature and rainfall patterns in Europe and North America. The yearly variability of the NAO makes it a predictor of future climate. For example, negative NAO values mainly reduce the disturbances directed toward the south, generating cold and dry winters in the northern Europe, snowfall in the USA, and increased precipitation in southern Europe (Martinez-Artigas et al. 2021).

The eastern zone of Andalusia is more influenced by the humid and warm flows coming from the Mediterranean, and thus it is more influenced by the teleconnection detectable using the West Mediterranean Oscillation (WeMO) index. In this zone, the torrential rains registered between September and November are related to the negative phase of the WeMO (Meseguer-Ruiz et al., 2021). Analyzing the links between these climatic indices and the magnitude of extreme events is useful for understanding cycles of repeatability (or return period) and forecasting risky periods in advance.

In Fig. 8, the extrapolation of the values of the mapped percentiles at the location of the preserved fortifications allows the classification of the hazard level for these types of heritage buildings. The fortifications indicated on the map with red circles (8.80%) have a higher probability of being strongly affected by extreme rainfall, especially considering that ongoing climate change is worsening the current conditions (Olcina 2020; P.R. Shukla et al. 2020). The increase in humidity and the erosive power of extreme rainfall are the main causes of degradation of these structures Beckett et al., 2020; Mileto et al., 2017), especially in the absence of preventive maintenance and conservation policies. The degradation processes triggered in these contexts include the appearance of pathologies such as moist areas, iron-rich patina, alveolation, and fissured or cavernized rocks that reinforce the base of the structures, efflorescence, and erosion of the bare wall. In extreme situations, they can cause the structures to bulge because of the expansion of the clays, the displacement, and the sanding alteration of the base (Bui et al. 2009; Moreno et al. 2019; Shao et al. 2013; Yun-xia et al. 2017).

#### 4.2.2. *Drought areas and their occurrences*

Andalusia is in a transitional area between the influences of polar and subtropical atmospheric circulations. This makes the precipitation patterns in this region complex, making it difficult to identify drought risk. The aridity derived from an evapotranspiration potential greater than that of rainfall during long periods without rain also makes the forecast of return periods of droughts difficult to assess (Torelló-Sentelles and Franzke, 2021; Peña et al., 2016).

The use of drought indices such as SPI is, therefore, very useful. At short time scales, (1–3 months) SPI is related to the soil moisture content, while at longer time scales (6 months and 1 year), it is related to the

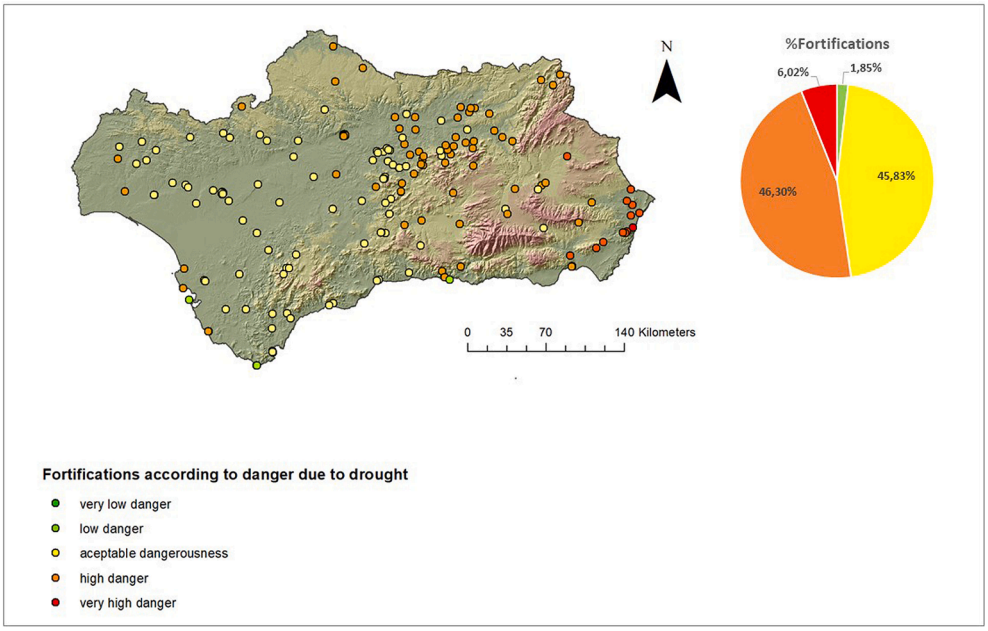


**Fig. 11.** Fortifications preserved in Andalusia classified according to danger of droughts as highlighted in the legend below. The percentage of fortification at different danger level is also reported as pie chart on the top right.

availability of groundwater. Fig. 9 shows that at a 12-month time scale, the SPI was reconstructed using precipitation data obtained by CHIRPS over the Andalusian region for the RP. From the long-term climate reconstructions available in the literature, it is evident that Andalusia has regularly experienced drought events over the recent decades. The results obtained allow us to compare the intensity, spatial extension, and frequency of meteorological drought registered in different zones of the analyzed region. Eight years during the RP presented moderate drought events (SPI ranging from –1.00 to –1.49) that affected a large part of the analyzed territory. Six years presented strong drought events (SPI from –1.49 to –2.00; orange color in the map) that affect more limited geographic areas. Finally, extreme drought events (SPI > –2.00; red color in the map) were identified in the eastern part of Andalusia in 1998 and 2005.

The low percentile maps (Fig. 10) allow the identification of areas of the territory that have been more intensely affected by droughts. The 10th percentile map indicates that for the entire Andalusian territory, the years analyzed contained moderate drought below 10% (SPI from –1.00 to –1.49; Fig. 9a). The 5th and 2nd percentile maps (Fig. 10b and 10c) make it possible to identify sub-areas with severe and extreme droughts i.e., being within the 5% and 2% of extreme events among all the data analyzed, respectively. These sub-areas most affected by droughts are identified in the eastern zone, corresponding to the sub-desert Mediterranean climate.

The modeled situation is especially alarming in the context of climate change. Climate models regionalized by the AEMET indicate an increase in evapotranspiration in semi-arid areas of the Mediterranean and predict a reduction in water resources in the years to come (CEDEX, 2017). Similar to the development of extreme precipitation events, the relationship between the periods of drought recorded in Andalusia and the teleconnection patterns has been highlighted by different authors, particularly highlighting the influence of WeMO and the East Atlantic/West Russia (EATL/WRUS) index (Mathbout et al. 2021). Although it exceeds the objectives of this research, deepening the knowledge of these relationships will allow forecasting future risk situations associated with severe drought events.

From a risk management point of view, identifying fortifications in environments that have been most affected by drought events over recent years is very useful. The degradation processes of rammed-earth fortifications in this environment include cracking of the walls and detachment. After intense rain, the external part of the mud walls undergoes a disintegration process that generates a slurry film. These films tend to detach during droughts due to the lack of humidity and high temperatures (Cui et al. 2019). In the presence of strong winds, periods of drought also generate strong erosion and sandblasting processes (Richards et al. 2020).

Fig. 11 shows the extrapolation of the drought values obtained by the analysis of the 2nd percentile of the SPI at the locations of the fortifications. As in the case of extreme rainfall events, the fortifications were classified into five groups according to the risk analysis. Of the fortifications analyzed, 6.02% were located in areas that were highly dangerous due to drought. Although the fortifications located in Almería (Southeast) will be the most affected by drought, there is a small group of fortifications located in the eastern coastal area of Andalusia that have a high risk of drought during the summer (Fig. 11) and a high risk of extreme rainfall in the winter (Fig. 8).

In conclusion, Fig. 12 shows the top 5 fortifications located in the most dangerous areas due to both extreme rainfall (blue-colored table in Fig. 12) and drought (red-colored table in Fig. 12). However, the type of remains preserved (rampart, settlement, castle, tower, etc.), construction technique used (monolithic or mixed rammed earth), and the present state of conservation of the fortification will also affect the level of risk they will be subjected to. Therefore, the proposed method is a part of a broader research work that also aims, in the next stages, to analyze vulnerability (Moreno et al. 2019) and risk at the heritage landscape scale.

## 5. Conclusions

The validation of the CHIRPS and PERSIANN satellite resources with the ground weather station located at the Seville Airport shows that these two resources, allowed to achieve a high precision but a low accuracy in the reconstruction of extreme rainfall values. Therefore, the readjustment of thresholds used in ground-based stations becomes necessary when comparing ground- and satellite-based data together.

Google Earth Engine allows access to preprocessed satellite images and joint analysis of large volumes of information. The comparison between massive and statistical analysis of data from satellite resources

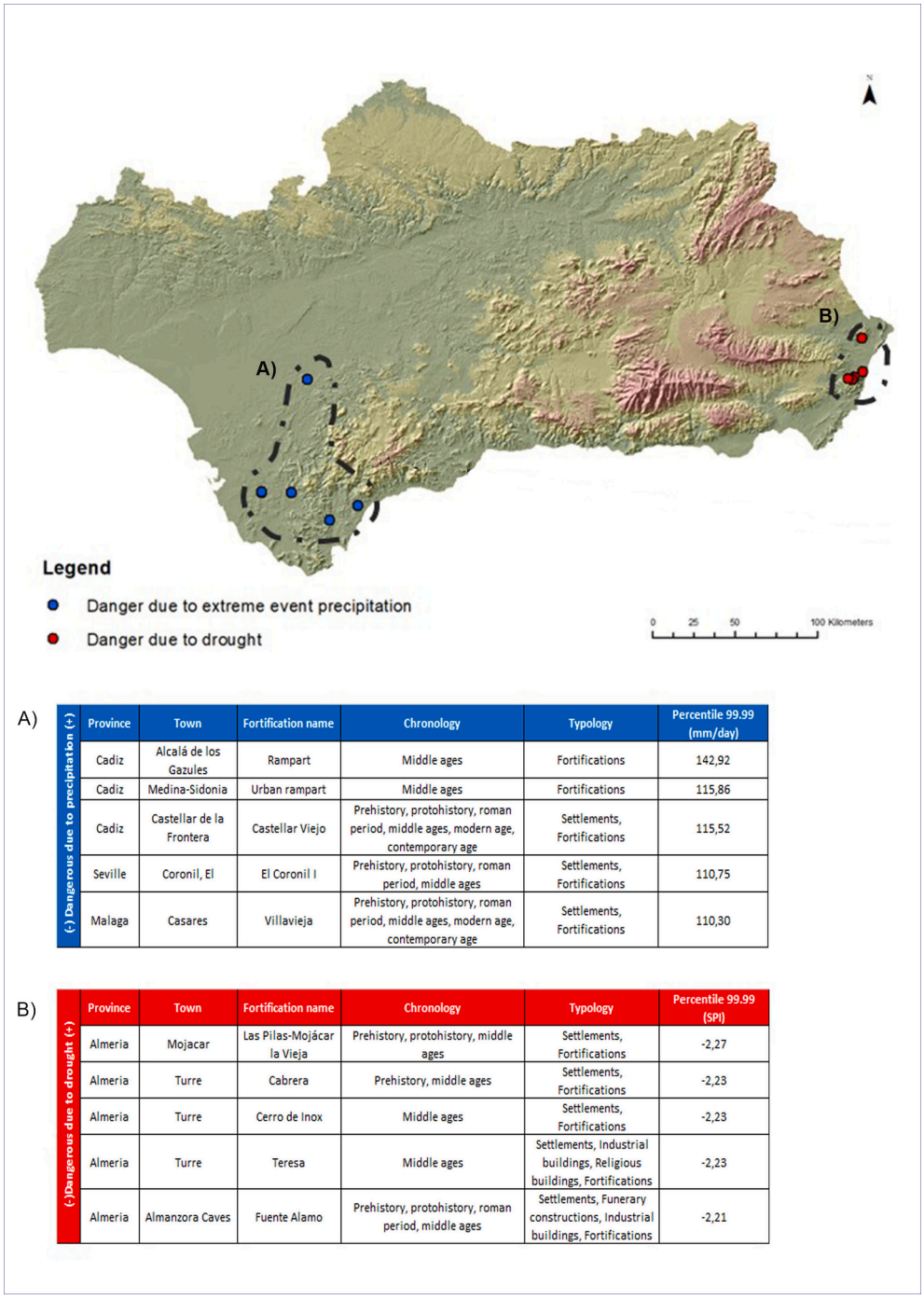


A)

(-) Dangerous due to precipitation (+)

| Province | Town | Fortification name | Chronology | Typology | Percentile 99.99 (mm/day) |
|---|---|---|---|---|---|
| Cadiz | Alcalá de los Gazules | Rampart | Middle ages | Fortifications | 142,92 |
| Cadiz | Medina-Sidonia | Urban rampart | Middle ages | Fortifications | 115,86 |
| Cadiz | Castellar de la Frontera | Castellar Viejo | Prehistory, protohistory, roman period, middle ages, modern age, contemporary age | Settlements, Fortifications | 115,52 |
| Seville | Coronil, El | El Coronil I | Prehistory, protohistory, roman period, middle ages | Settlements, Fortifications | 110,75 |
| Malaga | Casares | Villavieja | Prehistory, protohistory, roman period, middle ages, modern age, contemporary age | Settlements, Fortifications | 110,30 |

B)

(-)Dangerous due to drought (+)

| Province | Town | Fortification name | Chronology | Typology | Percentile 99.99 (SPI) |
|---|---|---|---|---|---|
| Almeria | Mojacar | Las Pilas-Mojácar la Vieja | Prehistory, protohistory, middle ages | Settlements, Fortifications | -2,27 |
| Almeria | Turre | Cabrera | Prehistory, middle ages | Settlements, Fortifications | -2,23 |
| Almeria | Turre | Cerro de Inox | Middle ages | Settlements, Fortifications | -2,23 |
| Almeria | Turre | Teresa | Middle ages | Settlements, Industrial buildings, Religious buildings, Fortifications | -2,23 |
| Almeria | Almanzora Caves | Fuente Alamo | Prehistory, protohistory, roman period, middle ages | Settlements, Funerary constructions, Industrial buildings, Fortifications | -2,21 |

**Fig. 12.** Fortifications located in the areas of highest danger due to droughts (red circles with information i.e. name, typology and chronology reported in the table with red header) and extreme rainfall (blue circles with information reported in the table with blue header).. (For interpretation of the references to color in this figure legend, the reader is referred to the web version of this article.)

and ground meteorological stations allows knowing the degree of confidence and precision of the different satellite resources over a specific territory. This aspect ensures a correct interpretation of the data and minimizes the uncertainty associated with the use of satellite precipitation products obtained from indirect measurements and predictive model.

To correct underestimations and define thresholds capable of detecting extreme events, the relative data were analyzed instead of absolute data. This analysis was based on big-data scale analysis of > 10,000 satellite images using percentile-type statistical reducers, indices, and map algebra. this approach together with the readjusted thresholds after validation with ground stations allowed the evaluation of rainfall recorded over the entire analyzed land cover (i.e., the Andalusia region in Spain) and the identification of the areas most affected by extreme rainfall and droughts.

This methodology can be easily replicated elsewhere based on available data from CHIRPS and ground weather stations. The simplicity of the model allows to join analysis with other hazard mapping, as well as the periodic updating of the information. Its use in the elaboration of risk maps, the development of warning systems, and predictive risk models has high potentiality to design a more efficient management plan and implementation of the conservation resources. In this way, using

elaborated cartography in applications such as risk or hydrological modeling sometimes requires resampling of pixel size to improve spatial resolution. In this case, the uncertainty and the errors dependent on the change of scale must be evaluated prior to the elaboration of the model (Hong et al., 2014; Wu and Li, 2009). The applicability of the proposed method of analysis to the Andalusia region demonstrated its reliability owing to the achieved results. In fact, the analysis was capable of detecting a range of extreme rainfall regimes that considerably differed between the eastern and western zones of the region. The observed trends underlined the development of extreme precipitation events (in terms of mm/day) occurring in the western zone under the influence of the North-South Atlantic teleconnection pattern. The fortifications located in this area can therefore be strongly affected by humidity problems, and erosion of the base after the occurrence of such extreme rainfall events.

In terms of the incidence of droughts, this method is also promising as it highlighted how the southeastern area, characterized by the presence of a sub-desert Mediterranean climate, has been the area most affected by droughts in recent years. The fortifications in this area can be strongly affected by fracturing, sandblasting, and detachment due to periods of drought.

Lastly, the links between these areas and the frequency of occurrence with the location of sites of the rammed-earth fortifications preserved in the region allowed the classification of the degree of danger in the surrounding landscape in relation to the analyzed hazard variables. Through our work, we were able to list fortifications in danger of extreme rainfall or drought.

The results presented are a part of a more complex research project on multivariable risk assessment of heritage landscapes. In this context, the proposed method allows to obtain climatic trends and extreme precipitation events by CHIRPS and PERSIANN (Ashouri et al., 2015; Hsu et al., 2021). Along with the use of satellite resources such as TRMM, GPM or GSMAP, capable of quantifying the force, duration, and intensity of a daily rain event (Funk et al., 2015; Tang et al., 2020), allows monitoring the hazard levels in the rainy season in heritage landscapes. In turn, the joint analysis of the vulnerability (Diaz et al., 2022; Moreno et al., 2019) and the hazards (Moreno et al., 2022) allows identifying points of greater risk and therefore must be intervened with higher urgency to avoid the loss of heritage structures.".

The maps obtained facilitate the handling of large volumes of satellite information and enable its addition as a cartographic base in multicriteria risk models created with Geographic Information Systems. It is especially useful in the case of earthen architecture in which the water access inside the structures is one of the main causes of degradation, as well as in archaeological sites that are exposed to inclement weather.

To sum up, the proposed model is a simple and useful tool to support risk mitigation and provide a better understanding of the time scale and of the locations/fortifications over which preventive conservation actions must be implemented, or extraordinary maintenance and adaptation actions must be planned and realized, for effective climate change impact and disaster risk reduction.

## Declaration of Competing Interest

The authors declare that they have no known competing financial interests or personal relationships that could have appeared to influence the work reported in this paper.

## Acknowledgements

This study has been carried out thanks to the methodology supported by the projects: Art-Risk (RETOS project of Ministerio de Economía y Competitividad and Fondo Europeo de Desarrollo Regional (FEDER), code: BIA2015-64878-R (MINECO/FEDER, UE)), Art-Risk cooperación: Conservación preventiva frente a rehabilitación de urgencia del Patrimonio Arquitectónico mediante Investigación sobre Riesgos y Vulnerabilidad frente al Cambio Climático, desastres naturales y antrópicos (project of Consejería de Fomento, Infraestructuras y Ordenación del Territorio, Junta de Andalucía UPO-03), FENIX (project of Ministerio de Ciencia e Innovación, Programas Estatales de Generación de Conocimiento y Fortalecimiento Científico y Tecnológico del Sistema de I + D + i, code: PID2019-107257RB-I00), Diagnóstico y Catalogación del Patrimonio Arquitectónico Andaluz mediante Análisis de Riesgos y vulnerabilidad (project of Consejería de fomento, infraestructuras y ordenación del territorio de la Junta de Andalucía UPO.20-01), RESILIENT-TOURISM project of Consejería de Transformación Económica, Industria, Conocimiento y Universidades. Junta de Andalucia (PYC20 RE 034 UPO), the research teams TEP-199 and Sanit-ARTE laboratory. The Art-Risk methodology has been awarded the Europa Nostra 2020 prize. M. Moreno is grateful to the State Program for the Promotion of Talent and its Employability in R + D + i of Ministerio de Ciencia e Innovación of Spain for his technical fellowship (PTA2019-016882) and for his research stay in the Norwegian University of Science and Technology (Norway).

## Bibliography

Abate, N., Lasaponara, R., 2019. Preventive Archaeology Based on Open Remote Sensing Data and Tools: The Cases of Sant'Arsenio (SA) and Foggia (FG) Italy. Sustain. (Switzerland) 11 (15). https://doi.org/10.3390/su11154145.

Agapiou, A., Lysandrou, V., Alexakis, D.D., Themistocleous, K., Cuca, B., Argyriou, A., Sarris, A., Hadjimitsis, D.G., 2015. Cultural Heritage Management and Monitoring Using Remote Sensing Data and GIS: The Case Study of Paphos Area, Cyprus. Comput. Environ. Urban Syst. 54 (November), 230–239. https://doi.org/10.1016/j.compenvurbsys.2015.09.003.

Agapiou, A., 2017. Remote Sensing Heritage in a Petabyte-Scale: Satellite Data and Heritage Earth Engine© Applications. Int. J. Digital Earth 10 (1), 85–102. https://doi.org/10.1080/17538947.2016.1250829.

Agapiou, A., Lysandrou, V., 2021. Observing Thermal Conditions of Historic Buildings through Earth Observation Data and Big Data Engine. Sensors 21 (13). https://doi.org/10.3390/S21134557.

Agapiou, A., Lysandrou, V., Hadjimitsis, D.G., 2020. Earth Observation Contribution to Cultural Heritage Disaster Risk Management: Case Study of Eastern Mediterranean Open Air Archaeological Monuments and Sites. Remote Sensing 12 (8). https://doi.org/10.3390/RS12081330.

AghaKouchak, A., Farahmand, A., Melton, F.S., Teixeira, J., Anderson, M.C., Wardlow, B. D., Hain, C.R., 2015. Remote Sensing of Drought: Progress, Challenges and Opportunities. Rev. Geophys. 53 (2), 452–480. https://doi.org/10.1002/2014RG000456.

Aktas, Y., 2021. Cities and Urban Heritage in the Face of a Changing Climate. Atmosphere 12 (8), 1007. https://doi.org/10.3390/ATMOS12081007.

Ambrosia, V. G., J. San Miguel-Ayanz, L. Boschetti, L. Giglio, & R. D. Field. 2019. "The Group on Earth Observation (GEO) Global Wildfire Information System (GEO-GWIS)." *AGUFM* 2019: NH12A-02. https://ui.adsabs.harvard.edu/abs/2019AGUFMNH12A..02A/abstract.

Avram, E., H. Guillaud, and M. Hardy. 2001. Characterization of Earthen Materials, in Terra Literature Review. An Overview of Research in Earthen Architecture Conservation.

Balti, H., Abbes, A.B., Mellouli, N., Riadh Farah, I., Sang, Y., Lamolle, M., 2020. A Review of Drought Monitoring with Big Data: Issues, Methods, Challenges and Research Directions. Ecol. Inf. 60 (November) https://doi.org/10.1016/J.ECOINF.2020.101136.

Barmpoutis, P., Papaioannou, P., Dimitropoulos, K., Grammalidis, N., 2020. A review on early forest fire detection systems using optical remote sensinG. Sensors (22), 6442. https://doi.org/10.3390/s20226442.

Beckett, C.T.S., Jaquin, P.A., Morel, J.C., 2020. Weathering the Storm: A Framework to Assess the Resistance of Earthen Structures to Water Damage. Constr. Build. Mater. 242 (May), 118098 https://doi.org/10.1016/J.CONBUILDMAT.2020.118098.

Brimblecombe, P., C. M. Grossi, & I. Harris. 2011. "Climate Change Critical to Cultural Heritage." In *Environmental Earth Sciences*, 195–205. Springer Verlag. https://doi.org/10.1007/978-3-540-95991-5_20.

Bonazza, A., Sardella, A., Kaiser, A., Cacciotti, R., et al., 2021. Safeguarding cultural heritage from climate change related hydrometeorological hazards in Central Europe. Int. J. Disaster Risk Reduction (63), 102455. https://doi.org/10.1016/J.IJDRR.2021.102455.

Bui, Q.B., Morel, J.C., Venkatarama Reddy, B.V., Ghayad, W., 2009. Durability of Rammed Earth Walls Exposed for 20 Years to Natural Weathering. Build. Environ. 44 (5), 912–919. https://doi.org/10.1016/J.BUILDENV.2008.07.001.

Cagigas, D. et al. 2020. "Registro Software: Art-Risk 3.0. Software Basado En Inteligencia Artificial Aplicada a La Conservación Preventiva de PH (Iglesias). SE-967-19, UPO, US e IVCR+i." 2020. https://www.upo.es/investiga/art-risk-service/art-risk3/index.html.

Camuffo, D., A. della Valle, & F. Becherini. 2020. "A Critical Analysis of the Definitions of Climate and Hydrological Extreme Events." *Quaternary International* 538 (October): 5–13. https://doi.org/10.1016/j.quaint.2018.10.008.

Cacciotti, R., Kaiser, A., Sardella, A., et al., 2021. Climate change-induced disasters and cultural heritage: optimizing management strategies in Central Europe. Clim. Risk Manage. (32), 100301. https://doi.org/10.1016/J.CRM.2021.100301.
Carroll, P., Aarrevaara, E., 2018. Review of Potential Risk Factors of Cultural Heritage Sites and Initial Modelling for Adaptation to Climate Change. Geosciences (Switzerland) 8 (9). https://doi.org/10.3390/geosciences8090322.
Casado, M.J., Pastor, M.A., Doblas-Reyes, F.J., 2010. Links between Circulation Types and Precipitation over Spain. Phys. Chem. Earth, Parts A/B/C 35 (9–12), 437–447. https://doi.org/10.1016/J.PCE.2009.12.007.
Centro de Estudios y experimentación de obras públicas (CEDEX). 2017. "Evaluación Del Impacto Del Cambio Climático En Los Recursos Hídricos y Sequías En España." Madrid.
Chuvieco, E. 2016. "Fundamentals of Satellite Remote Sensing: An Environmental Approach.".
Chuvieco, E., 2007. Mirar Desde El Espacio o Mirar Hacia Otro Lado: Tendencias En Teledetección. Documents d'Anàlisi Geogràfica. https://www.raco.cat/index.php/DocumentsAnalisi/article/view/86622.
Council of Europe. 2009. *European Landscape Convention and Reference Documents*. www.coe.int/Conventioneuropeennedupaysage.
Criado-Aldeanueva, F., Soto-Navarro, J., 2020. Climatic Indices over the Mediterranean Sea: A Review. Appl. Sci. 10 (17), 5790.
Cuca, B., 2017. "The Contribution of Earth Observation Technologies to Monitoring Strategies of Cultural Landscapes and Sites". *International Archives of the Photogrammetry*. Remote Sens. Spatial Inf. Sci. ISPRS Arch. 42 (2W5), 135–140. https://doi.org/10.5194/ISPRS-ARCHIVES-XLII-2-W5-135-2017.
Cuca, B., Hadjimitsis, D.G., 2019. Space technology meets policy: an overview of Earth Observation sensors for monitoring of cultural landscapes within policy framework for Cultural Heritage. J. Archaeol. Sci.: Rep. (14), 727–733. https://doi.org/10.1016/j.jasrep.2017.05.001.
Cui, K., Du, Y., Zhang, Y., Wu, G., Yu, L., 2019. An Evaluation System for the Development of Scaling off at Earthen Sites in Arid Areas in NW China. Heritage Sci. 7 (1) https://doi.org/10.1186/s40494-019-0256-z.
Dastgerdi, A.S., Sargolini, M., Pierantoni, I., 2019. Climate change challenges to existing cultural heritage policy. Sustainability 11 (19), 5227.
Denis, G., Pasco, X., 2015. The challenge of future space systems and services in Europe: industrial competitiveness without a level playing field. Defense Ind. (4), 44–58. https://doi.org/10.1089/space.2013.0034.
Diaz, G.A., Ortiz, R., Moreno, M., Ortiz, P., 2022. Vulnerability Assessment of Historic Villages in the Amazonas Region (Peru). International Journal of Architectural Heritage 16 (5). https://doi.org/10.1080/15583058.2022.2070049.
Elfadaly, A., Abutaleb, K., Naguib, D., Lasaponara, R., 2022. Detecting the environmental risk on the archaeological sites using satellite imagery in Basilicata region, Italy. Egypt. J. Remote Sens. Sp. Sci. 25 (1), 181–193.
Fatorić, S., Seekamp, E., 2017. Are Cultural Heritage and Resources Threatened by Climate Change? A Systematic Literature Review. Clim. Change 142 (1–2), 227–254. https://doi.org/10.1007/s10584-017-1929-9.
Fernanda, M[a], & P. López. 2003. "El Clima de Andalucia." In *Geografía de Andalucia*, edited by A López Ontiveros, 137–74.
Figueiredo, R., Romão, X., Paupério, E., 2020. Flood Risk Assessment of Cultural Heritage at Large Spatial Scales: Framework and Application to Mainland Portugal. J. Cult. Heritage 43 (May), 163–174. https://doi.org/10.1016/j.culher.2019.11.007.
Gandini, A., L. Garmendia, & R. San Mateos. 2017. "Towards Sustainable Historic Cities: Adaptation to Climate Change Risks." Edited by Manuela Tvaronavičienė. Entrepreneurship Sustain. Issues 4 (3): 319–27. https://doi.org/10.9770/jesi.2017.4.3S(7).
Funk, C., Peterson, P., Landsfeld, M., et al., 2015. The climate hazards infrared precipitation with stations: a new environmental record for monitoring extremes. Sci. Data 2 (1), 1–21.
Gao, Y., Skutsch, M., Paneque-Gálvez, J., Ghilardi, A., 2020. Remote sensing of forest degradation: a review. Environ. Res. Lett. 15 (10), 103001.
García-Barrón, L., Aguilar-Alba, M., Morales, J., Sousa, A., 2018. Intra-Annual Rainfall Variability in the Spanish Hydrographic Basins. Int. J. Climatol. 38 (5), 2215–2229. https://doi.org/10.1002/JOC.5328.
Ghamisi, P., Rasti, B., Yokoya, N., et al., 2019. Multisource and multitemporal data fusion in remote sensing: a comprehensive review of the state of the art. IEEE Geosci. Remote Sens. Magaz. 7 (1), 6–39.
Gómez-Zotano, J., Alcántara-Manzanares, J., Olmedo-Cobo, J.A., Martínez-Ibarra, E., 2015. La Sistematización Del Clima Mediterráneo: Identificación, Clasificación y Caracterización Climática de Andalucía (España). Revista de Geografía Norte Grande 61, 161–180. https://scielo.conicyt.cl/scielo.php?pid=S0718-34022015000200009&script=sci_arttext.
Google Developers: Get Started with Earth Engine, 2022. https://developers.google.com/earth-engine/getstarted. (Accessed 09 January 2022).
Gorelick, N., Hancher, M., Dixon, M., et al., 2017. Google Earth Engine: Planetary-scale geospatial analysis for everyone. Remote Sens. Environ. 202, 18–27. https://doi.org/10.1016/j.rse.2017.06.031.
Guttman, N.B., 1999. Accepting the Standardized Precipitation Index: A Calculation Algorithm. J. Am. Water Resour. Assoc. 35 (2), 311–322. https://doi.org/10.1111/j.1752-1688.1999.tb03592.x.
Hadjimitsis, D., Agapiou, A., Alexakis, D., Sarris, A., 2013. Exploring Natural and Anthropogenic Risk for Cultural Heritage in Cyprus Using Remote Sensing and GIS. Int. J. Digital Earth 6 (2), 115–142. https://doi.org/10.1080/17538947.2011.602119.
Hadjimitsis, D. G, K. Themistocleous, B. Cuca, A. Agapiou, V. Lysandrou, R. Lasaponara, N. Masini, & G. Schreier. 2020. *Remote Sensing for Archaeology and Cultural Landscapes : Best Practices and Perspectives Across Europe and the Middle East*. Edited by Themistocleous Kyriacos Cuca Branka, Agapiou Athos Lysandrou Vasiliki, Lasaponara Rosa Masini Nicola, and Schreier Gunter. http://www.springer.com/series/10182.
Heim, R., 2002. A Review of Twentieth-Century Drought Indices Used in the United States. Bull. Am. Meteorol. Soc. 83 (8), 1149–1166. https://doi.org/10.1175/1520-0477-83.8.1149.
Holloway, J., Mengersen, K., 2018. Statistical machine learning methods and remote sensing for sustainable development goals: a review. Remote Sens. 10 (9), 1365.
Hong, Y., Zhang, Y., Weng, Q., 2014. Spatiotemporal scales of remote sensing precipitation. Scale Issues Remote Sens. John Wiley & Sons, New Yersey, pp. 253–267.
Hsu, J., Huang, W., Liu, P., Li, X., 2021. Validation of CHIRPS precipitation estimates over Taiwan at multiple timescales. Remote Sens. 13 (2), 254. https://doi.org/10.3390/RS13020254.
Jiao, W., Wang, L., McCabe, M.F., 2021. Multi-Sensor Remote Sensing for Drought Characterization: Current Status, Opportunities and a Roadmap for the Future. Remote Sens. Environ. 256 (April), 112313 https://doi.org/10.1016/J.RSE.2021.112313.
Kumar, L., Mutanga, O., 2018. Google Earth Engine Applications since Inception: Usage, Trends, and Potential. Remote Sensing 10 (10). https://doi.org/10.3390/rs10101509.
Lasaponara, R., Masini, N., 2020. Big Earth Data for Cultural Heritage in the Copernicus Era. In Remote Sens. Archaeol. Cultural Landscapes 31–46. https://doi.org/10.1007/978-3-030-10979-0_3.
Levin, N., Ali, S., Crandall, D., Kark, S., 2019. World Heritage in Danger: Big Data and Remote Sensing Can Help Protect Sites in Conflict Zones. Global Environ. Change 55 (March), 97–104. https://doi.org/10.1016/j.gloenvcha.2019.02.001.
Liu, Q., Zhang, S., Zhang, H., Bai, Y., Zhang, J., 2020. Monitoring Drought Using Composite Drought Indices Based on Remote Sensing. Sci. Total Environ. 711 (April), 134585 https://doi.org/10.1016/J.SCITOTENV.2019.134585.
Lopez, T., Al Bitar, A., Biancamaria, S., Güntner, A., Jäggi, A., 2020. On the Use of Satellite Remote Sensing to Detect Floods and Droughts at Large Scales. Surv. Geophys. 41 (6), 1461–1487. https://doi.org/10.1007/S10712-020-09618-0.
Luo, L., Wang, X., Guo, H., Lasaponara, R., Zong, X., Masini, N., Wang, G., Shi, P., Khatteli, H., Chen, F., Tariq, S., Shao, J., Bachagha, N., Yang, R., Yao, Y.a., 2019. Airborne and spaceborne remote sensing for archaeological and cultural heritage applications: a review of the century (1907–2017). Remote Sens. Environ. 232, 111280.
Ma, Y., Wu, H., Wang, L., Huang, B., Ranjan, R., Zomaya, A., Jie, W., 2015. Remote Sensing Big Data Computing: Challenges and Opportunities. Future Gener. Comput. Syst. 51 (October), 47–60. https://doi.org/10.1016/j.future.2014.10.029.
Maierhofer, Ch, Ch Köpp, S Kruschwitz, M Drdacky, Ch Hennen, S Lanza, M Tomaževič, et al. 2008. *Cultural Heritage Protection against Flood-A European FP6 Research Project*.
Martin-Vide, J., Albert Lopez-Bustins, J., 2006. The Western Mediterranean Oscillation and Rainfall in the Iberian Peninsula. Int. J. Climatol. 26 (11), 1455–1475. https://doi.org/10.1002/joc.1388.
Martinez-Artigas, J., Lemus-Canovas, M., Albert Lopez-Bustins, J., 2021. Precipitation in Peninsular Spain: Influence of Teleconnection Indices and Spatial Regionalisation. Int. J. Climatol. 41 (S1), E1320–E1335. https://doi.org/10.1002/JOC.6770.
Mathbout, S., Albert Lopez-Bustins, J., Royé, D., Martin-Vide, J., 2021. Mediterranean-Scale Drought: Regional Datasets for Exceptional Meteorological Drought Events during 1975–2019. Atmosphere 12 (8). https://doi.org/10.3390/atmos12080941.
McKee, TB, NJ Doesken, & J Kleist - Proceedings of the 8th, and undefined 1993. 1993. "The Relationship of Drought Frequency and Duration to Time Scales." *Climate. Colostate.Edu*, 17–22. https://climate.colostate.edu/pdfs/relationshipofdroughtfrequency.pdf.
Meseguer-Ruiz, O., Lopez, J.A., Arbiol, L., et al., 2021. Temporal changes in extreme precipitation and exposure of tourism in Eastern and South-Eastern Spain. Theor. Appl. Climatol. 144 (1), 379–390.
Michaelides, S., Levizzani, V., Anagnostou, E., Bauer, P., Kasparis, T., Lane, J.E., 2009. Precipitation: Measurement, Remote Sensing, Climatology and Modeling. Atmos. Res. 94 (4), 512–533. https://doi.org/10.1016/J.ATMOSRES.2009.08.017.
Ministerio de Medio Ambiente, y Medio Rural y Marino. Agencia Estatal de Meteorología. 2011. *ATLAS CLIMÁTICO IBÉRICO IBERIAN CLIMATE ATLAS GOBIERNO DE ESPAÑA*. Madrid.
Mileto C, & F. Vegas López Manzanares. 2017. Proyecto COREMANS.Criterios de Intervención En La Arquitectura de Tierra / The COREMANS Project. Intervention Criteria for Earthen Architecture. Madrid: Ministerio de Educación, Cultura y Deporte. https://es.calameo.com/read/0000753354317 21e39425.
Moreno, M., Ortiz, R., Cagigas-Muñiz, D., et al., 2022. ART-RISK 3.0 a fuzzy—based platform that combine GIS and expert assessments for conservation strategies in cultural heritage. J. Cult. Herit. (55), 263–276. https://www.sciencedirect.com/science/article/pii/S1296207422000632.
Moreno, M., Ortiz, P., Ortiz, R., 2019. Vulnerability Study of Earth Walls in Urban Fortifications Using Cause-Effect Matrixes and Gis: The Case of Seville, Carmona and Estepa Defensive Fences. Mediterranean Archaeol. Archaeometry 19 (3), 119–138. https://doi.org/10.5281/zenodo.3583063.
Mutanga, O., Kumar, L., 2019. Google earth engine applications. Remote Sens. 11 (5), 591. https://doi.org/10.3390/rs11050591.
Olcina, J., 2020. Clima, Cambio Climático y Riesgos Climáticos En El Litoral Mediterráneo. Oportunidades Para La Geografía. Documents d'Anàlisi Geogràfica 66 (1), 159. https://doi.org/10.5565/rev/dag.629.
Organización Meteorológica Mundial. 2012. *Índice Normalizado de Precipitación - Guía Del Usuario*.
Organización Meteorológica Mundial, 2020. Guía del Sistema Mundial de Observación. OMM.

Orr, S.A., Richards, J., Fatorić, S., 2021. "Climate Change and Cultural Heritage: A Systematic Literature Review (2016–2020)". *The Historic Environment: Policy & Practice*. Historic Environ. Policy Pract. 12 (3-4), 434–477.

P.R. Shukla, J. Skea, R. Slade, S. Connors, E. Vyas, & Huntley k. 2020. *An IPCC Special Report on Climate Change, Desertification, Land Degradation, Sustainable Land Management, Food Security, and Greenhouse Gas Fluxes in Terrestrial Ecosystems*. Edited by IPCC.

Phillips, H., 2015. The Capacity to Adapt to Climate Change at Heritage Sites—The Development of a Conceptual Framework. Environ. Sci. Policy 47 (March), 118–125. https://doi.org/10.1016/J.ENVSCI.2014.11.003.

Quattrochi, D.A., Wentz, E., Lam, N.S.N., Emerson, C.W., 2017. Integrating scale in remote sensing and GISWeng, Quiao (Ed.), In: Series in Remote Sensing applications. CRC Press, New York.

Richards, J., Viles, H., Guo, Q., 2020. The Importance of Wind as a Driver of Earthen Heritage Deterioration in Dryland Environments. Geomorphology 369 (November), 107363. https://doi.org/10.1016/J.GEOMORPH.2020.107363.

Peña, M., S. R. Gámiz, A. Y. Castro, & M.J. Esteban-Parra. 2016. "Análisis Comparativo de Índices de Sequía En Andalucía Para El Periodo 1901-2012." *Cuadernos de Investigación Geográfica / Geographical Research Letters, ISSN 0211-6820, ISSN-e 1697-9540, Nº 42, 1, 2016, Págs. 67-88* 42 (42): 67–88. https://doi.org/10.18172/cig.2946.

Sabbioni, C, P Brimblecombe, & M Cassar. 2010. *THE ATLAS OF CLIMATE CHANGE IMPACT ON EUROPEAN CULTURAL HERITAGE Scientific Analysis and Management Strategies NOAH'S ARK GLOBAL CLIMATE CHANGE IMPACT ON BUILT HERITAGE AND CULTURAL LANDSCAPES*. www.anthempress.com.

Rossler, M., 2006. World heritage cultural landscapes: a UNESCO flagship programme 1992–2006. Landsc. Res. 31 (4), 333–353.

Sahoo, A.K., Sheffield, J., Pan, M., Wood, E.F., 2015. Evaluation of the Tropical Rainfall Measuring Mission Multi-Satellite Precipitation Analysis (TMPA) for Assessment of Large-Scale Meteorological Drought. Remote Sens. Environ. 159 (March), 181–193. https://doi.org/10.1016/J.RSE.2014.11.032.

Schär, C., Ban, N., Fischer, E.M., Rajczak, J., Schmidli, J., Frei, C., Giorgi, F., Karl, T.R., Kendon, E.J., Tank, A.M.G.K., O'Gorman, P.A., Sillmann, J., Zhang, X., Zwiers, F.W., 2016. Percentile indices for assessing changes in heavy precipitation events. Clim. Change 137 (1-2), 201–216.

Sesana, E., Gagnon, A.S., Ciantelli, C., Cassar, JoAnn, Hughes, J.J., 2021. Climate Change Impacts on Cultural Heritage: A Literature Review. WIREs Clim Change 12 (4). https://doi.org/10.1002/wcc.710.

Shao, M., Li, L.i., Wang, S., Wang, E., Li, Z., 2013. Deterioration Mechanisms of Building Materials of Jiaohe Ruins in China. J. Cult. Heritage 14 (1), 38–44. https://doi.org/10.1016/J.CULHER.2012.03.006.

Sun, Q., Miao, C., Duan, Q., Ashouri, H., Sorooshian, S., Hsu, K.L., 2018. A Review of Global Precipitation Data Sets: Data Sources, Estimation, and Intercomparisons. Rev. Geophys. 56 (1), 79–107. https://doi.org/10.1002/2017RG000574.

Themistocleous, K. 2020. "The Use of UAVs for Cultural Heritage and Archaeology." In *Remote Sensing for Archeology and Cultural Landscapes*, edited by Hadjimitsis D., 18: 241–69. Springer, Cham. https://doi.org/10.1007/978-3-030-10979-0_14.

Tang, G., Clark, M.P., Papalexiou, S.M., et al., 2020. Have satellite precipitation products improved over last two decades? A comprehensive comparison of GPM IMERG with nine satellite and reanalysis datasets. Remote Sens. Environ. 240, 111697. https://doi.org/10.1016/J.RSE.2020.111697.

Taylor, K., St Clair, A., Mitchell, N., 2014. Conserving Cultural Landscapes. UNESCO. https://whc.unesco.org/en/news/1194 (Accessed 09 January 2022).

Torelló-Sentelles, H., Franzke, C., 2021. Drought impact links to meteorological drought indicators and predictability in Spain. Hydrol. Earth Syst. Sci. Discuss. 1–32 https://doi.org/10.5194/HESS-2021-209.

Toth, C., Jóźków, G., 2016. Remote Sensing Platforms and Sensors: A Survey. *ISPRS J. Photogramm. Remote Sens.*. Elsevier B.V. 115, 22–36.

UNESCO. 2020. *Recommendation on the Historic Urban Landscape: Report of the Second Consultation on Its Implementation by Member States, 2019*. Paris. https://whc.unesco.org/uploads/activities/documents/activity-638-98.pdf.

Vishwakarma, B. D. 2020. "Monitoring Droughts From GRACE." *Frontiers in Environmental Science* 8 (December). https://doi.org/10.3389/FENVS.2020.584690.

Wang, X., & L. Luo. 2020. "From Remote Sensing Archaeology to Space Archaeology: A New Task in the Era of Cultural Heritage Protection." *Yaogan Xuebao/Journal of Remote Sensing*. Science Press. https://doi.org/10.11834/jrs.20200016.

Wang, H., Xu, Z., Fujita, H., Liu, S., 2016. Towards felicitous decision making: an overview on challenges and trends of Big Data. Inf. Sci. 367, 747–765.

Weiss, M., Jacob, F., Duveiller, G., 2020. Remote sensing for agricultural applications: a meta-review. Remote Sens. Environ. 236, 111402.

Wellmann, T., Lausch, A., Andersson, E., Knapp, S., Cortinovis, C., Jache, J., Scheuer, S., Kremer, P., Mascarenhas, A., Kraemer, R., Haase, A., Schug, F., Haase, D., 2020. Remote Sensing in Urban Planning: Contributions towards Ecologically Sound Policies? Landscape Urban Plann. 204, 103921.

West, H., Quinn, N., Horswell, M., 2019. Remote Sensing for Drought Monitoring & Impact Assessment: Progress, Past Challenges and Future Opportunities. Remote Sens. Environ. 232 (October), 111291 https://doi.org/10.1016/J.RSE.2019.111291.

World Meteorological Organization. 2016. *GUIDELINES ON THE DEFINTION AND MONITORING OF EXTREME WEATHER AND CLIMATE EVENTS*.

Wilson, H., 2019. The Future of Our Pasts: Engaging cultural heritage in climate action Outline of Climate Change and Cultural Heritage. ICOMOS, Paris.

Wu, H., Li, Z.L., 2009. Scale issues in remote sensing: a review on analysis, processing and modeling. Sensors 9 (3), 1768–1793.

Xiao, W., Mills, J., Guidi, G., Rodríguez-Gonzálvez, P., Gonizzi Barsanti, S., González-Aguilera, D., 2018. Geoinformatics for the Conservation and Promotion of Cultural Heritage in Support of the UN Sustainable Development Goals. ISPRS J. Photogrammetry Remote Sens. 142 (August), 389–406. https://doi.org/10.1016/j.isprsjprs.2018.01.001.

Xu, X., Xie, F., Zhou, X., 2016. Research on spatial and temporal characteristics of drought based on GIS using Remote Sensing Big Data. Cluster Comput 19 (2), 757–767.

Yun-xia, S., Wen-wu, C., Jing, K., Wei-fei, D., 2017. Effect of Salts on Earthen Materials Deterioration after Humidity Cycling. J. Cent. South Univ 24, 796–806. https://doi.org/10.1007/s11771-017-3482-0.

Zargar, A, R Sadiq, B Naser, & FI Khan - Environmental Reviews, and undefined 2011. 2011. "A Review of Drought Indices." Cdnsciencepub.Com 19 (1): 333–349. https://doi.org/10.1139/A11-013.